CHAPTER 2

ELECTRODE/ELECTROLYTE INTERFACES: STRUCTURE AND KINETICS OF CHARGE TRANSFER

2.1. DOUBLE LAYER AT ELECTRODE/ELECTROLYTE INTERFACES

2.1.1. Structure, Charge, and Capacitance Characteristics

When a metal is partly immersed in an electrolyte, a potential is set up across the two phases, i.e., at the electrode/electrolyte interface. The phases may be solids (metals or alloys, semiconductors, insulators), liquids (ionic liquids, molten salts, neutral solutions), or gases (polar or non polar). The more common terminology in electrochemistry is that a *double layer* is set up at the interface. There are several reasons for a potential difference being set up across the interface of two phases, the most common one being the charge transfer occurring across the interface. During this process, a charge separation will occur because of electron transfer across the interface. Other reasons for the occurrence of potential differences are due to surface-active groups in the ionizable media (liquid, solid, or gas) and orientation of permanent or induced dipoles. The double layer at the interface between two phases has *electrical*, *compositional*, and *structural* characteristics. The electrical and compositional characteristics deal with the excess charge densities on each phase and the structural one with the distribution of the constituents (ions, electrons, dipoles, and neutral molecules) in the two phases, including the interfacial region. For the purposes of understanding and analyzing the electrical, compositional, and structural aspects relevant to the electrochemical reactions that occur in fuel cells, a

---

This chapter was written by S. Srinivasan.

brief description of the evolution of the theoretical aspects of the structure of the double layer, as applied to electrode/electrolyte interfaces, across which charge-transfer reactions occur, is presented in this section.

2.1.1.1. *Parallel-Plate Condenser Model: Helmholtz Model.*[1] This was the first type of model proposed for the structure of the double layer at an electrode/electrolyte interface. It is analogous to that in a solid-state capacitor—i.e., two layers of charge of opposite sign are separated by a fixed distance (Figure 2.1a). In this case, one may assume electrons in the metal and positive ions in solution. The potential drop across the interface will be linear and the capacitance ($C_{M\text{-}2}$) of the double layer is, as in the case of a parallel-plate condenser, given by:

$$C_{M-2} = \frac{\varepsilon}{4\pi d} \tag{2.1}$$

where ε is the dielectric constant in the medium between the plates and d is the distance between them. Assuming $\varepsilon = 6$ and $d = 3$ Å, the value of $C_{M\text{-}2}$ can be expected to be about 18 μF cm^{-2}. For the Helmholtz model, the differential and integral capacity are equivalent and have a constant value, even when there is a change in the charge density on the two layers (electrode and electrolyte).

However, what is measured experimentally is the differential capacity and one finds that this capacity varies with potential (Figure 2.2). This poses a question as to whether the model of fixed charges on the two layers constituting the double layer is valid, and therefore, it leads to the second model.

2.1.1.2. *Diffuse-Layer Model: Gouy*[2] *and Chapman*[3] *Model.* According to Gouy and Chapman, ions in the electric double layer are subjected to electrical and thermal fields. This allows the Maxwell-Boltzmann statistics to be applied to the charge distribution of ions as a function of distance away from the metal surface akin to the distribution of negatively charged ions surrounding a positive ion (Figure 2.1b). The analysis in both cases is similar except that for in the ion-ion case there is spherical symmetry, while for the electrode/electrolyte layers, it is planar. For this model, the diffuse charge (q_D) for a 1-1 electrolyte is given by:

$$q_D = \left(\frac{2kTn_0\varepsilon}{\pi}\right)^{1/2} \sinh\frac{e_0V}{2kT} \tag{2.2}$$

and the differential capacity, $C_{2\text{-}b}$, by:

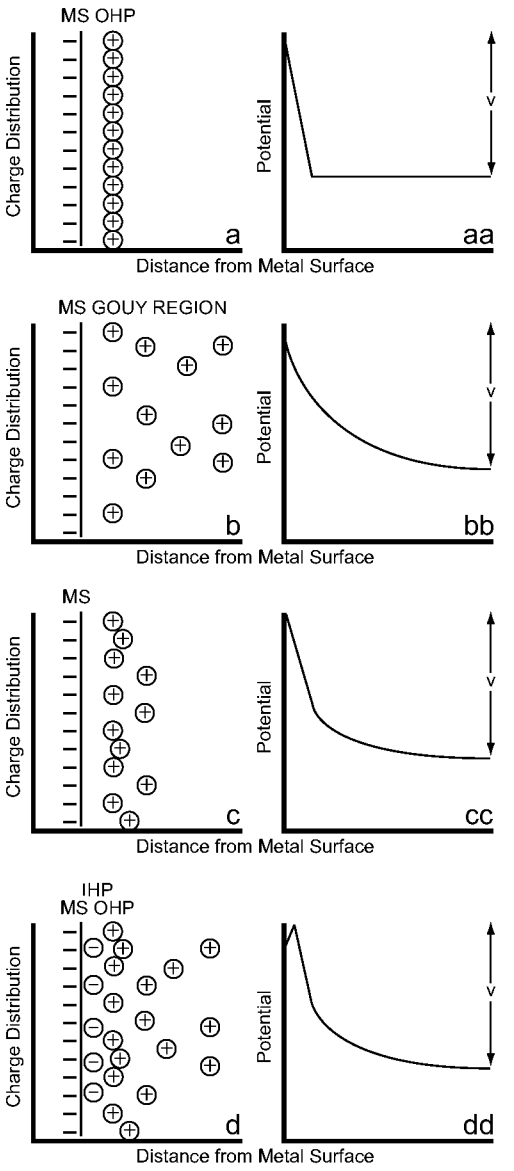

Figure 2.1. Evolution of the models of the double layer at electrode/electrolyte interface. Charge distribution vs. distance and potential variation vs. distance: (a) and (aa) Helmhotz model; (b) and (bb) Gouy-Chapman model; (c) and (cc) Stern model, and (d) and (dd) Esin and Markov, Grahame, and Devanathan model. Reprinted from Cited Reference 1 in Chapter 1.

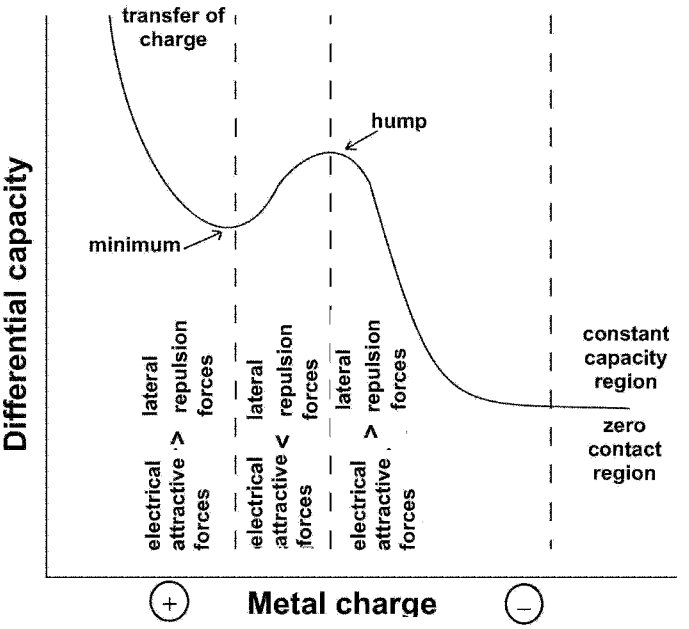

Figure 2.2. The lateral-repulsion model for the analysis of the capacity vs. potential plot. Reprinted from J. O'M. Bockris, A. K. N. Reddy, and Maria Gamboa-Aldeco, Modern Electrochemistry, Vol. 2A, 2nd edition. Copyright © 2000, with permission from Kluwer/Plenum Publishers.

$$C_{2-b} = \left(\frac{n_0 \varepsilon {e_0}^2}{2\pi kT} \right)^{1/2} \cosh \frac{e_0 V}{2kT} \tag{2.3}$$

where n_0 is the number of ions of positive and negative sign per unit volume in the bulk of the electrolyte and V is the potential drop from the metal to the bulk of the electrolyte.

According to this model, the capacitance is a minimum at $V = 0$ and rises to very high values symmetrically and parabolically on either side of $V = 0$. A typical potential-distance (from the electrode surface) plot for this model is presented in Figure 2.1bb. This model also had deficiencies because: (a) the experimental capacity-potential relations did not behave in a symmetrical-parabolic manner, except at potentials close to the potential of zero charge of the metal and in very dilute solutions; (b) it neglected ion-ion interactions which become increasingly

important at higher concentrations; and (c) it assumed a constant value of the dielectric constant in the region between the electrode and electrolyte.

2.1.1.3. *Compact Diffuse-Layer Model: Stern[4] Model.* This model is a hybrid one, consisting of the above two models. First, ions are considered to have a finite size and are located at a finite distance from the electrode. Second, the charge distribution in the electrolyte is divided into two contributions: (i) as in the Helmholtz model immobilized close to the electrode, and (ii) as in the Gouy-Chapman model, diffusely spread out in solution (Figure 2.1c). Thus,

$$q_M = Q_s = q_H + q_G \tag{2.4}$$

where q_M is the charge on the metal. Q_s is the total charge on the solution side (of opposite sign) comprising the Helmholtz fixed charge, q_H, and the Gouy-Chapman diffuse charge, q_G. The potential drops may be represented by:

$$V_M - V_{el} = (V_M - V_H) + (V_H - V_{el}) \tag{2.5}$$

where the subscripts *M, H,* and *el* denote the electrode, the Helmholtz layer on the solution side, and bulk electrolyte, respectively. As in the Helmholtz model, there is a linear variation of potential with distance across the Helmholtz component and a semi-exponential variation in the Gouy-Chapman component of the double layer (Figure 2.1cc). By differentiating Eq. (2.5) with respect to the charge, it can be shown that the double layer capacitance across this electrode/electrolyte interface is given by:

$$\frac{1}{C} = \frac{1}{C_H} + \frac{1}{C_G} \tag{2.6}$$

where C_H and C_G are the contributions of the Helmholtz and Gouy-Chapman capacitances, which are in series. There are two implications of this model. One is that in concentrated electrolytes the value of C_H^{-1} is considerably greater than that of C_G^{-1}. This model is very similar to that of Helmholtz (i.e., most of the charge is concentrated in the Helmholtz layer). The other implication is that in extremely dilute solution, $C_G^{-1} >> C_H^{-1}$ and therefore, $C = C_G$. Thus, the double-layer structure approaches that of the Gouy-Chapman model. This model shows reasonable values of C vs. V relations for electrolytes with non-adsorbable ions such as Na^+ or F^-. However, it is not applicable for electrolytes with specifically adsorbable anions as it cannot describe the differential capacity data shown in Figure 2.2. Furthermore, this model does not take into account the role of the solvent as related to the hydration of the ions and its influence on the structure of the double layer.

2.1.1.4. *Triple-Layer Model: Esin and Markov,[5] Grahame,[6] and Devanathan[7] Model.* The subtle feature of this model (Figure 2.1d), proposed by the three groups, was to take into consideration that ions could be dehydrated in the direction of the metal and specifically adsorbed on the electrode. Thus, an *inner layer* between the electrode surface and the Helmholtz layer further modifies the structure of the double layer. This inner layer is the locus of centers of unhydrated ions strongly attached to the electrode. For this case, Devanathan derived the relation:

$$\frac{1}{C} = \frac{1}{C_{M-1}} + \left(\frac{1}{C_{M-2}} + \frac{1}{C_{2-b}} \right) \left(1 - \frac{dq_1}{dq_M} \right) \tag{2.7}$$

where $C_{M\text{-}1}$ and $C_{M\text{-}2}$ are the integral capacities of the space between the electrode and the inner Helmholtz plane (IHP) and between the inner and outer Helmholtz planes (OHP), $C_{2\text{-}b}$ is the differential capacity of the diffuse double layer, and (dq_1/dq_M) represents the rate of change of the specifically adsorbed charge with charge on the metal. Some interesting analyses may be obtained from Eq. (2.7):

- If (dq_1/dq_M) is zero, the expression for the capacity (C) is equivalent to that for 3 capacitors in series, that is, inner Helmholtz, outer Helmholtz, and Gouy. Hence, this model is referred to as the *triple-layer model.*
- The capacity is a minimum when dq_1/dq_M is zero, because the latter can have only positive values.
- If dq_1/dq_M exceeds unity, the differential capacity attains large values. When C tends to infinity, the electrode becomes non-polarizable.
- The minimum in the capacity is in the vicinity of the potential of zero charge.

Specific adsorption of ions occurs because of different types of electrical interactions between the electrodes and ions: electric field forces, image forces, dispersion forces, and electronic or repulsive forces. When the image and dispersion forces are larger than the electronic force, the specific adsorption of ions occurs (*physical adsorption*). However, a stronger bond could be formed by partial electron transfer between the ion and the electrode (*chemisorption*); small cations (e.g., Na^+) have a strong hydration sheath around them and are minimally adsorbed. On the other hand, large anions (Cl^-, Br^-) have only a few water molecules in the primary hydration sheath and since the ion-solvent interaction in this case is considerably less than the above mentioned ion-electrode interaction, specific adsorption of the ions occurs with some partial charge transfer of an electron. The variation of potential with distance, across the electrode/electrolyte interface (Figure 2.1dd), reveals a steep drop between the electrode and IHP and then a small rise between the IHP and OHP, and thereafter the variation is similar to that in the diffuse layer.

2.1.1.5. *Water-Dipole Model: Bockris-Devanathan-Muller[8] Model.* For the above described models, the structure of the double layer is based on the interfacial charge characteristics of the electrode and of the ionic species in the

electrolyte. However, in electrochemistry, the bulk of the charge-transfer reactions occur in aqueous media. There are, of course, reactions in non-aqueous media such as organic solvents, molten salts, and solid electrolytes. The solvents like water or organic liquids (e.g., methanol, acetonitrile) are polar in character and contribute to the potential drop across the electrode/electrolyte interface. Thus, an innovative model for the structure of the double layer was proposed by Bockris, Devanathan, and Muller, which is schematically represented in Figure 2.3. The principal feature of this model is that, because of a strong interaction between the charged electrode and water dipoles, there is a strongly held, oriented layer of water molecules attached to the electrode. In this layer, because of competitive adsorption, there could also be some specifically adsorbed ions which are possible partially solvated. The locus of centers of these ions is the *inner Helmholtz plane* (IHP).

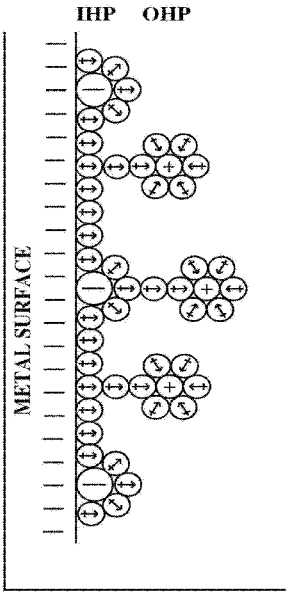

Figure 2.3. Water dipole model of the double layer at an electrode/electrolyte interface, (Bockris, Devanathan and Muller). Reprinted from Reference 8, Copyright © 1963, with permission from the Royal Society of London.

Adjacent to this layer is the layer of solvated ions, which is the locus of centers of the hydrated ions, i.e., the outer Helmholtz plane (OHP). Next to this layer is the diffuse layer, which is predominant in dilute electrolytes. Just as in the case of a primary hydration sheath surrounding an ion, the first layer of water molecules has a strong orientation (either parallel or anti-parallel to the electric field depending on the charge of the metal). Such a complete orientation yields a dielectric constant of about 6 for this layer. Next to this layer is a second layer of water molecules, somewhat disoriented due to electrical and thermal forces (this is similar to the secondary hydration sheath around an ion). This layer has a dielectric constant of about 30 to 40. The succeeding layers of water molecules behave like bulk water, which has a dielectric constant of *ca.* 80.

2.1.2. Effect of Specific Adsorption of Ions on the Double Layer Structure and their Adsorption Isotherms

Using the Bockris-Devanathan-Muller model (water-dipole model), the constant capacity on the negative side of the capacity-potential plot can be rationalized. The interpretation of the variation of capacity with potential at less negative and positive potentials is more complex and is dealt with in detail in the revised edition of the book *Modern Electrochemistry*. For the purpose of this chapter as well as its relevance to interfaces at which fuel cell reactions occur, a brief analysis of the regions of the capacitance-potential plot is presented next.

2.1.2.1. *The Region of Constant Capacity at Negative Potentials.* This is attributed to the Helmholtz type double layer and is not affected by the nature of ions in the double layer. The capacity thus attains a constant value of about 16 μF cm^{-2} at the mercury electrode/electrolyte interface. It must be noted that higher values will be observed on metals, even if polished and smooth, because of some degree of roughness of these metals, as compared with mercury.

2.1.2.2. *Capacity Hump.* As illustrated in Figure 2.2, with an increase of potential in the positive direction, there is an increase of capacity leading to a maximum (*capacity hump*), followed by a decrease to a minimum, and then a sharp increase. For an explanation of this behavior, it is necessary to examine the general expression for the capacity at an electrode/electrolyte interface:

$$\frac{1}{C} = \left(\frac{1}{K_{M-OHP}}\right) - \left(\frac{1}{K_{M-OHP}} - \frac{1}{K_{M-IHP}}\right)\left(\frac{dq_{ca}}{dq_M}\right) \tag{2.8}$$

where $K_{M\text{-}OHP}$ and $K_{M\text{-}IHP}$ refer to the integral capacity of the M-OHP and M-IHP regions, respectively.

If $(dq_{ca}/dq_M) \rightarrow 0$, the capacity will be a constant, but the limiting case will not be when there is no contact adsorption of ions. This equation also shows that C

increases when q_{ca} increases with q_M, i.e., the capacity increases with potential difference across the double layer. The increase occurs until the electrode charge becomes positive, the extent of specific adsorption further increases and then the rate of its growth decreases. The question then is: Why is there this rate of decrease? The answer is that apart from the chemical and electrical forces that promote specific adsorption of ions, ion-ion lateral interaction forces play a role with increasing coverage of the electrode surface by the specifically adsorbed ions. Thus, there is the hump or a maximum in the differential capacity vs. the metal charge plot (Figure 2.2). After this decrease in capacity, there is again a sharp rise in the capacity, and this is due to the strong interaction between the highly, positively charged metal and the specifically adsorbed negatively charged ion. It has been demonstrated that the specific adsorption of the ions in this region of potential could also involve a partial charge transfer between the ion and the electrode. The above description shows that the specific adsorption of ions affects the structure of the double layer, which is reflected in the variation of the differential capacity with potential. It also has the effect on the variation of potential across the double layer with distance (Figure 2.1aa). A third effect is that specifically adsorbed ions can block sites for electrochemical reactions on the surfaces of the electrodes. Thus, knowledge of the adsorption behavior of these ions as a function of potential and/or charge on the metal is essential in elucidating the kinetics of electrode reactions. The adsorption behavior of ions on electrodes has been elucidated following an approach similar to that used in heterogeneous catalysis, and involves the adsorption of reactants, intermediates, and/or products on the surfaces of the catalysts. Common terminology is to express the adsorption behavior as *adsorption isotherms*, which are essentially equations of state relating physical quantities to the extent of adsorption. For example, if one considers the adsorption of an anion, A^-, on an electrode, M, in the equilibrium state, as represented by

$$A^-_{sol} + M \underset{\leftarrow}{\overset{\rightarrow}{}} MA^-_{sol} \tag{2.9}$$

the corresponding chemical potentials (μ) can be written as,

$$\mu_{A_{sol}} = \mu^0_{A_{sol}} + RT \ln a \tag{2.10}$$

and

$$\mu_{MA_{ads}} = \mu^0_{MA_{ads}} + RT \ln f(\theta) \tag{2.11}$$

where a is the activity of the ions A^- in solution and $f(\theta)$ is some function of the coverage of the electrode by the adsorbed species, θ. In order to find an expression for $f(\theta)$, it is necessary to have knowledge of the type of adsorption and for this, several types of adsorption isotherms have been proposed. The oldest is the Langmuir isotherm,[9] and in this case it is assumed that for the reaction represented

by Eq. (2.9), the *rate of adsorption* (ν_1) is proportional to the free surface on the electrode. Thus,

$$\nu_1 = k_1(1-\theta)a_{A_{sol}} \tag{2.12}$$

where k_1 is the rate of the adsorption reaction. The *rate of the desorption* reaction (ν_{-1}) is given by:

$$\nu_{-1} = k_{-1}\theta \tag{2.13}$$

where k_{-1} is the rate of the reverse reaction. Under equilibrium conditions,

$$\nu_1 = \nu_{-1} \tag{2.14}$$

and

$$\frac{\theta}{1-\theta} = (\frac{k_1}{k_{-1}})a_{A^-} \tag{2.15}$$

Frumkin (1925) considered lateral interactions of the adsorbed species and the expression for the adsorption isotherm was modified to:[10]

$$\frac{\theta}{1-\theta}\exp(-2A\theta) = \frac{k_1}{k_{-1}}a_{A^-} \tag{2.16}$$

where

$$A = -\frac{N_a\varphi_a}{2kT} \tag{2.17}$$

and φ_a is the interaction energy of one molecular pair and $N_a\varphi_a$ is the interaction energy of one molecule with N_a nearest neighbors. A positive value of A arises when there is attraction of the adsorbed particles and a negative value results for repulsion.

Temkin (1941) assumed heterogeneity of the surface but no molecular interactions, and for this case the adsorption isotherm is expressed by:[11]

$$\theta = \frac{1}{f}\ln\beta_0 a_{A^-} \tag{2.18}$$

where $f = K/kT$ with K being a constant and $\beta_0 = W\exp(Q/kT)$ where W is a parameter related to the distribution of molecules in solution and in the adsorbed state, and Q to the enthalpy of adsorption.

In the Flory[12]-Huggins[13] type of isotherm, it was assumed that the adsorption process involves the displacement of water molecules from the surface, i.e.,

$$A^-_{sol} + nH_2O_{ads} \underset{\leftarrow}{\overset{\rightarrow}{}} A_{ads} + nH_2O_{sol} \tag{2.19}$$

The resulting isotherm has the form:

$$\frac{\theta}{(1-\theta)^n} e^{(1-n)} = \beta A^-_{sol} \tag{2.20}$$

A more generalized form of the isotherm for the specific adsorption of ions, developed by Bockris, Gamboa-Aldeco, and Szklarczyk,[14] takes into account surface heterogeneity, solvent displacement, charge transfer, lateral interactions, and ion size. The expression for this isotherm is:

$$\theta = \frac{1}{f}\left(-\frac{\Delta G_{ch,i}}{kT} - \frac{\Delta G_{ch,w}}{kT} - \frac{\Delta G_E}{kT} - \frac{\Delta G_L}{kT} + \frac{f}{2} + \ln\frac{c}{c_w} \right) \tag{2.21}$$

where $\Delta G_{ch,i}$ and $\Delta G_{ch,w}$ represent the chemical part, ΔG_E, the potential dependent part, ΔG_L the lateral part of the free energy change for the adsorption of the ion, and c and c_w the bulk concentration of the ion and water in the solution, respectively. The term f is equal to $-2v_0/kT$, where v_0 is an energy parameter of the lattice. This equation was tested with the experimental results for adsorption of chloride and bisulfate ions on platinum and the agreement was quite good (Figure 2.4). Knowledge of such type of adsorption behavior of ions is essential in an analysis of the kinetics of the electrode reactions because ionic adsorption can block sites for the reaction and can also affect the potential distribution across the electrode/electrolyte interface.

2.1.3. Effect of Adsorption of Neutral Molecules on the Structure of the Double Layer

An understanding of the adsorption behavior of neutral molecules (mainly organics) is also essential in elucidating the reaction kinetics across electrode/electrolyte interfaces, particularly in the low to intermediate temperature range in aqueous electrolytes. The significance of the effects of organic adsorption in electrochemical energy conversion (fuel cells) cannot be overstated because adsorption of species like carbon monoxide and of intermediates formed during the electrooxidation of organic fuels, such as methanol, causes significant overpotential

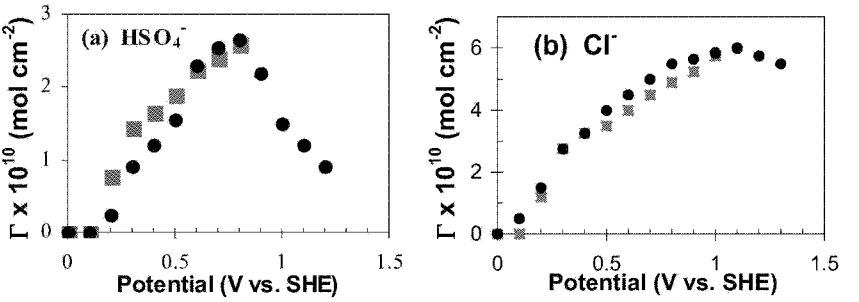

Figure 2.4. Adsorption of (a) chloride ions (b) bisulfate ions on platinum as a function of potential. Reprinted from Reference 14, Copyright © (1992), with permission from Elsevier.

(polarization) losses at the anodes in these fuel cells. Since the 1920s, it has been realized that the potential dependence of adsorption of organic species on an electrode is essentially parabolic in behavior (Figure 2.5).[15] The water-dipole model or the structure of the double layer provides an explanation for this behavior in the

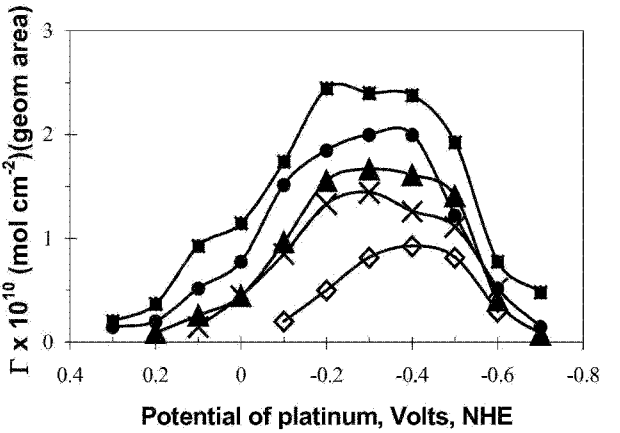

Figure 2.5. Typical coverage vs. potential plot for adsorption of an organic compound (naphthalene) on an electrode at an interface with electrolyte. Case illustrated is for adsorption of napthalene on platinum for different bulk concentrations of naphthalene in the electrolyte: (■) $1x10^{-4}$ M, (●) $5x10^{-5}$ M, (▲) $1x10^{-5}$ M, (×) $5x10^{-6}$ M, and (◊) $2.5x10^{-6}$ M. Reprinted from Reference 15, Copyright © (1964), with permission from The Electrochemical Society, Inc.

following manner. The strong interaction between the water dipole and the electrode is mainly due to the electric field at the electrode/electrolyte interface, but there is also a small contribution to the electric field at the electrode/electrolyte interface due to the chemical interaction of the water molecule with the electrode. The electric field causes the orientation of the water molecules on either side of *the potential of zero charge* (pzc), i.e., if the electrode is negatively charged the positive end of the water dipole will be oriented towards the electrode and vice versa. The weakest interaction between the electrode and the water molecule is at a potential close to the pzc. It is for this reason that a pseudo-symmetrical inverse relation is observed for the variation of extent of adsorption with potential across the interface—i.e., the maximum adsorption is at a potential close to the pzc and there is a steady decrease in the extent of adsorption on either side of the pzc.[1]

Research studies on the behavior of organic adsorption in electrochemistry are quite extensive. Organic adsorption plays key roles not only in electrochemical energy conversion, but also in electroorganic synthesis, corrosion protection, electrodeposition, electrochemical sensors, etc. Apart from the adsorption behavior being controlled by the dependence of the orientation of the water molecules, organic adsorption depends on the chemical interaction between the organic molecules and the electrode surface (for example, the π orbital interaction of aromatics with the electrode) and charge-transfer reactions, which could occur between the organic species and the electrode.

In general, organic adsorption may be represented by a displacement of adsorbed water molecules according to the reaction:

$$[\text{organic}]_{\text{sol}} + n\text{H}_2\text{O}_{\text{ads}} \rightleftarrows [\text{organic}]_{\text{ads}} + n\text{H}_2\text{O}_{\text{sol}} \tag{2.22}$$

There could also be an adsorption via charge transfer and the adsorbed species could be without or with any breakdown in the chemical structure, the latter being an intermediate during an electron transfer reaction. Just as in the case of ionic adsorption, the adsorption behavior of organic species can be expressed in terms of adsorption isotherms (Langmuir, Frumkin, Temkin, Flory-Huggins, Bockris-Gamboa-Aldeco-Szklarczyk, etc.). A generalized isotherm was developed by Bockris and Jeng[16] by considering the adsorption process as a solvent substitution process, and the water molecules being adsorbed in three configurations as monomers in flipped-up and flopped-down positions and as dimers with no net dipole as described by

$$\begin{aligned}[\text{organic}]_{\text{sol}} + o[\text{H}_2\text{O}]\uparrow + p[\text{H}_2\text{O}]\downarrow + q[\text{H}_2\text{O}]\uparrow\downarrow \\ \rightleftarrows [\text{organic}]_{\text{ads}} + (o+p+2q)\text{H}_2\text{O}_{\text{sol}}\end{aligned} \tag{2.23}$$

[1] The maximum does not occur exactly at the pzc because of the difference in chemical interactions between the electrode and the water molecules that depend on whether the H or the O atom is oriented towards the metal.

Comparison of the adsorption behavior of n-valeric acid (an aliphatic compound) and phenol on platinum with theory (Figure 2.6) reveals that the maxima in the coverage-potential curve are in the vicinity of the pzc. The factors, which affect adsorption of organic compounds/species on electrodes, may be summarized as follows:

- Aliphatic hydrocarbons, linear or branched, interact weakly with the electrode or water molecules, and thus the extent and strength of their adsorption is small. However, if the aliphatic molecules have functional groups (CO, CO-NH_2), they interact with water molecules and the surface of the electrode, and also have higher amounts of potential dependent adsorption.
- Aromatic compounds generally have π electron interactions with neighboring atoms and with electrodes and these exhibit potential dependent adsorption. Further, unlike linear aliphatic molecules, which are vertically oriented when adsorbed on the electrode, aromatics at low coverage have a flat orientation on the electrode (see Figure 2.6 for comparison). Similarly, unsaturated linear compounds tend to have an orientation with the multiple bonds parallel to the surface. At higher coverages of the aromatics, there could be a reorientation in the vertical position to accommodate more molecules.

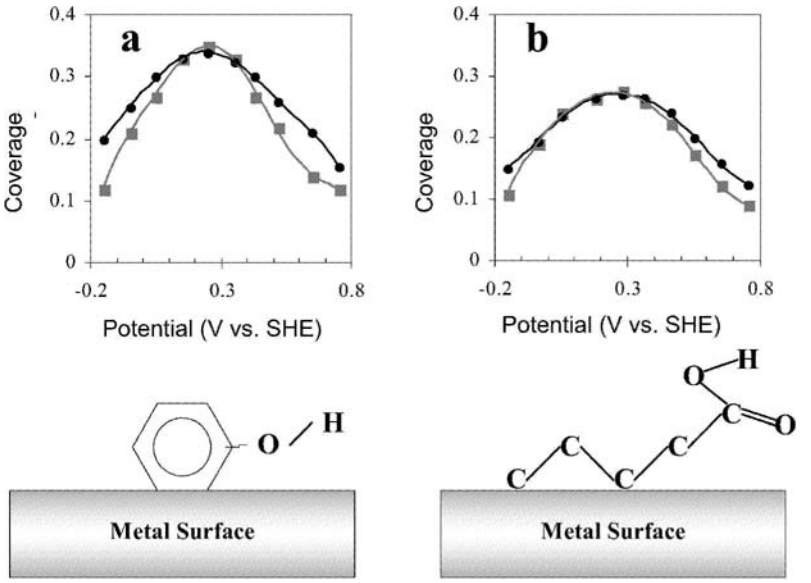

Figure 2.6. Comparison of coverage vs. potential for phenol and valeric acid on platinum. Reprinted from Reference 16, Copyright © (1992), with permission from Elsevier.

- The morphology of the electrode surface also affects the adsorption characteristics. The extent of adsorption appears to be less on rough surfaces than on smooth ones and on the former, there is less reorientation (horizontal to vertical) of adsorbed aromatic molecules.
- The electrolyte also affects organic adsorption. Organic molecules are, in general, considerably larger in size than the ions. Thus, more water molecules adsorbed on the electrode will have to be displaced. In addition, the organic molecules will have to be dissociated from any water molecules with which they are hydrated because they have polar groups. In general, the lower the solubility of the organic compound in the electrolyte, the higher the adsorbability on the electrode.

This short description of the extensive topic of the adsorption behavior of organic compounds on electrodes signifies its important role in affecting the characteristics of the double layer across electrode/electrolyte interfaces. Adsorption of organic compounds (i) affects the electric field across the interface; (ii) blocks sites for the desired electron transfer across the interface; and (iii) poisons electrode surfaces with strongly adsorbed species such as CO from reformed fuels or formed as intermediates during electrooxidation of organic fuels. For more details on this topic, the reader can refer to the revised edition of the book *Modern Electrochemistry,* Vol. 2A by Bockris, Reddy, and Gamboa-Aldeco.

2.1.4. Brief Analysis of Structures of Semiconductor/Electrolyte and Insulator/Electrolyte Interfaces

Semiconductor/electrolyte and insulator/electrolyte interfaces are also often encountered in electrochemical systems. They are of particular relevance to (i) photo-electrochemical reactions for use of solar energy to produce hydrogen and oxygen at semiconductor/electrolyte interfaces, and (ii) colloid and interfacial phenomena at insulator/electrolyte interfaces. Figure 2.7 schematically represents the potential distribution of a semiconductor electrode/electrolyte interface.

There are three characteristic regions. The regions across the interface (B-C) and that into the bulk (C-D) of the electrolyte are analogous to that for a metal/electrolyte interface. It is the region A-B, the *space-charge region*, which is different. It extends to a considerable distance within the semiconductor; for a carrier concentration of 10^{14} electrons cm^{-3}, and it is about 10^{-4} cm. The variation of potential with distance is similar to that in the diffuse-layer region. The charged species, which contributes to the potential distribution in the space charge region, are electrons, holes, or may be immobile impurity ions. Brattain and Garrett, who were the first to investigate the double layer characteristics of semiconductor/electrolyte interfaces,[17] used an approach similar to that of Gouy and Chapman. A major part of the potential drop is within the semiconductor in region A-B, which is unlike the case of the metal/electrolyte interface, where it is in the

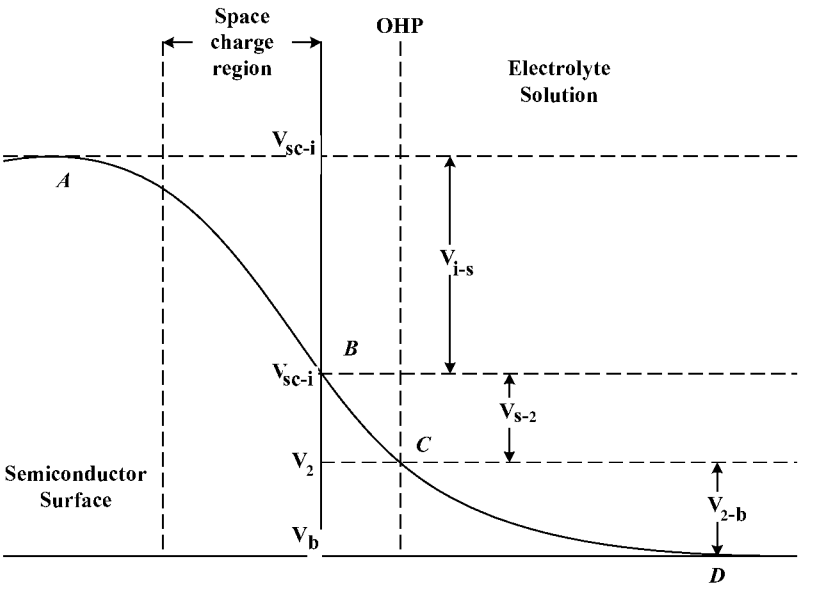

Figure 2.7. Potential distribution across semiconductor/electrolyte interface. Reprinted from J. O'M Bockris and S. Srinivasan, *Fuel Cells: Their Electrochemistry*, Copyright © 1969, with permission from McGraw Hill Book Company, with permission of The McGraw-Hill Companies.

Helmholtz layer. The equivalent circuit for the semiconductor/electrolyte circuit consists of three capacitors in series, and thus the overall capacity can be expressed by:

$$\frac{1}{C} = \frac{1}{C_{SC}} + \frac{1}{C_H} + \frac{1}{C_{dl}} \tag{2.24}$$

where the subscripts *SC*, *H* and *dl* represent the space charge layer, Helmholtz layer, and the Gouy layer, respectively. It must be noted that in this simple model, electrons become trapped in the surface, whereby quantum states for electrons on the surface differ from that in the bulk causing surface states. In the presence of surface states, the potential variation within the semiconductor resembles that of the double layer across a metal-electrolyte interface with the specific adsorption of ions.

When there is a movement of one phase relative to the other, electrokinetic phenomena arise because of the presence of a surface charge on the insulator material. Just as in the case of metals and semiconductors, there is some interaction of the surface charge species in the insulator material and ionic and dipolar species in the electrolyte. Specific adsorption of ions could also play a role. Studies have

shown that the potential drop across the insulator material/electrolyte interface is significant in very dilute electrolytes. An important parameter in electrokinetic phenomena is the *zeta potential* (ξ) across the insulator/electrolyte interface, defined as the potential drop from the shear plane to the bulk of the electrolyte. It is somewhat less than the potential drop in the Gouy region at an interface between a metal and an electrolyte. The zeta potential is a valuable parameter in the sense that we can calculate free surface charge characteristics of the insulator material by using an equation similar to that in the Gouy-Chapman theory relating the diffuse-layer potential to the surface charge.

Zeta potentials can be measured in four different ways. If the insulator material is in the form of a narrow tube or porous plug, a flow of the electrolyte under pressure (P) gives rise to a *streaming potential* (E) or *streaming current* (i). The zeta potential (ξ) is calculated from the slope of the streaming potential-pressure plot according to the relation:

$$\xi = \frac{4\pi\eta\kappa}{\varepsilon}\left(\frac{dE}{dP}\right) \tag{2.25}$$

where η, κ and ε are the viscosity, specific conductance, and dielectric constant of the electrolyte.

The reverse of this electrokinetic phenomenon is the *electroosmostic flow*. In this case, a passage of current through the tube or porous plate the causes the flow of electrolyte from one end to the other. The zeta potential can be calculated from the expression:

$$\xi = \frac{4\pi\eta\kappa\nu}{\varepsilon i} \tag{2.26}$$

where η,κ, and ε are as defined above, ν is the rate of flow, and i is the current passing through the tube or porous plug.

Extensive studies related to electrokinetic phenomena have been made with colloidal particles (inorganic, organic, and biological). Two types of measurement are made, i.e., *electrophoresis* and *sedimentation potential*. Electrophoresis is the migration of colloidal particles in an electrolyte under the influence of an electric field. The zeta potential may be calculated from the *electrophoretic mobility* (ν), according to the equation:

$$\xi = \frac{4\pi\eta\nu}{\varepsilon E} \tag{2.27}$$

where E is the electric field in the electrolyte. This technique has been widely used to determine the surface charge characteristics of colloidal *isoelectric* points (i.e., the pH at which the ξ potential is zero), and the effect of dispersing or

agglomerating agents on the surface charge characteristics. The sedimentation potential method has been used only to a limited extent to determine surface charge characteristics. In this case, the colloidal particles are allowed to fall through a vertical column and the potential difference between two electrodes, vertically separated, is measured. The zeta potential across the colloid particle-electrolyte interface is given by the expression:

$$\xi = \frac{3\eta\kappa E}{\varepsilon\gamma^3(\rho - \rho')ngl} \tag{2.28}$$

where γ is the radius of the colloidal particles, ρ and ρ' are the densities of the particles and of the solution respectively, n is the number of particles in a unit volume, g is the acceleration due to gravity, l is the distance between the electrodes, and E is the sedimentation potential.

2.2. VITAL NEED FOR MULTI-DISCIPLINARY APPROACH

A wide variety of charge-transfer reactions occur at the interfaces of electrodes and electrolytes. The electrode materials could be metals or alloys, semiconductors, or enzymes. For practically all the types of reactions mentioned earlier, the electrolyte is aqueous. However, there are several cases in which the electrolytes are non-aqueous (e.g., ionizable inorganic or organic compounds, molten or solid state ionic conductors). An attempt is made in Figure 2.8 to represent the needed multi-disciplinary approach for investigation of the mechanisms of charge-transfer reactions.

Thermodynamics lay the groundwork to determine whether a charge-transfer reaction can occur spontaneously or needs to be driven using electrical energy. A charge-transfer reaction involves either the donation or acceptance of electrons by the electrode to or from a species in the electrolyte or adsorbed on the surface of the electrode. Since the electron has a very low mass and the thickness of the double layer is of the order of a few angstroms, the transfer of electrons occurs by quantum mechanical tunneling. Physical chemistry plays a significant role in elucidating the kinetics and electrocatalysis of the charge-transfer reactions. It is for this reason that electrode kinetics has been conventionally treated as a topic in physical chemistry, particularly in European countries. But just like material science, electrode kinetics embodies a multitude of disciplines. Statistical mechanical treatments of reaction rates have been most helpful, particularly in studies of reactions involving chemisorption of reactants and intermediates, as well as isotopic reactions. Metallurgy and solid-state science are involved in investigations of effects of electronic and geometric factors (crystal structure, defects) on electrocatalysis and their role in nucleation and crystal growth. The link between electrochemistry and surface science has been growing by leaps and bounds,

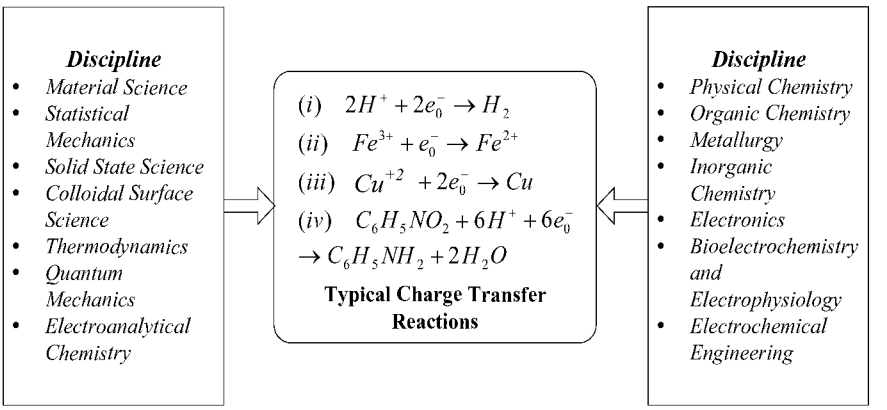

Figure 2.8. Multidisciplinary approaches for investigations of mechanisms of charge-transfer reactions.

particularly by the use of highly sophisticated *in situ* electrochemical/spectroscopic techniques, specifically for the examination of reactants, intermediates, and products adsorbed on surfaces, and the formation of passive films. Other techniques that are useful are Scanning Tunneling Microscopy (STM) and Atomic Force Microscopy (AFM) to examine electrodeposition or electrodissolution processes. Electrochemistry and material science are often grouped together because the structure, composition, and characteristics of the electrode material and solid electrolytes play key roles during the course of the charge-transfer reactions. They also depend on the methods of preparation of these materials; further, in electrocatalysis, the application of nanostructured materials is gaining momentum. Electronics is governed by solid-state electrochemistry. Charge-transfer reactions at electrode/electrolyte interfaces involve the physics of current flow and electric fields.

The progress made in electronics has been beneficial in designing circuitry to control potentials across interfaces as well as to investigate transient behavior, employing techniques such as electrochemical impedance spectroscopy. From a technological point of view, electrochemical engineering plays a major role toward understanding mass transport (diffusion, convection), hydro-dynamics of flow of solutions, transport of ions to surfaces, process control, etc. Last, but not least, bioelectrochemical charge transfer processes involve the disciplines of biochemistry and electrophysiology. Charge-transfer reactions in these systems are fascinating and involve both electron and proton transfer. The electrochemical mechanisms, by which biological systems function with respect to energy metabolism and nerve transmission, obey electrochemical laws. Their high efficiency and high speed can hardly be matched by simple organic or inorganic charge-transfer reactions.

2.3. SINGLE AND MULTI-STEP REACTIONS

Electrochemical reactions are similar to chemical reactions with one major difference: at least one step in the overall electrochemical reaction, the electron transfer reaction occurs across the electrode/electrolyte interface. In the case of chemical or biochemical reactions, there are three types of reactions: *single-step*, *consecutive-step*, and *parallel* reactions. Examples of these types of reactions are as follows:

- *Single-step reactions*. The electrodeposition/dissolution of a metal-like lithium occurs in a single step:

$$Li^+ + e_0^- \leftrightarrow Li \tag{2.29}$$

  This is the reaction occurring in a secondary lithium ion battery. Even though the reaction is represented by Eq. (2.29) in a single step, the electrodeposition step is followed by nucleation, surface diffusion of lithium, and crystal growth. In general, the kinetics of this reaction are relatively simple.
- *Consecutive-step reactions*. In a consecutive reaction, two or more intermediate steps occur in series, i.e., an intermediate produced in the first step is consumed in the second; if more than two intermediate steps are involved, the species produced in the second step takes part in the third step, etc. An example of this reaction of relevance to fuel cells is the four-electron transfer electroreduction of oxygen to water. A possible reaction pathway of this reaction on a platinum electrode in acid medium is:

$$O_2 + M + H_3O^+ + e_0^- \rightarrow MHO_2 + H_2O \tag{2.30}$$

$$MHO_2 + M \rightarrow MO + MOH \tag{2.31}$$

$$MO + H_3O^+ + e_0^- \rightarrow MOH + H_2O \tag{2.32}$$

$$2MOH + 2H_3O^+ + 2e_0^- \rightarrow 2M^+ + 4H_2O \tag{2.33}$$

  The overall reaction is, thus,

$$O_2 + 4H_3O^+ + 4e_0^- \rightarrow 6H_2O \tag{2.34}$$

  where *M* represents the electronically conducting electrode material (say Pt) and is not involved in the overall reaction. It plays the role of an electrocatalyst for the reaction. It must be noted that the intermediate step

represented by Eq. (2.33) occurs in two identical consecutive steps; the reason for this is that electron transfer occurs by quantum mechanical tunneling, which involves only one electron transfer at a time.

- *Parallel-step reactions.* When multistep reactions take place there is the possibility of parallel-intermediate steps. The parallel-step reactions could lead to the same final product or to different products. These types of reactions are more often encountered in electroorganic chemistry and bioelectrochemistry than in electrochemical reactions involving inorganic reactants and products. A fuel cell reaction, which sometimes exhibits this behavior, is the direct electrooxidation of organic fuels, such as hydrocarbons or alcohols. For instance, in the case of methanol, a six-electron transfer complete oxidation to carbon dioxide can occur consecutively in six or more consecutive steps; in addition, partially oxidized reaction products could arise producing formaldehyde and formic

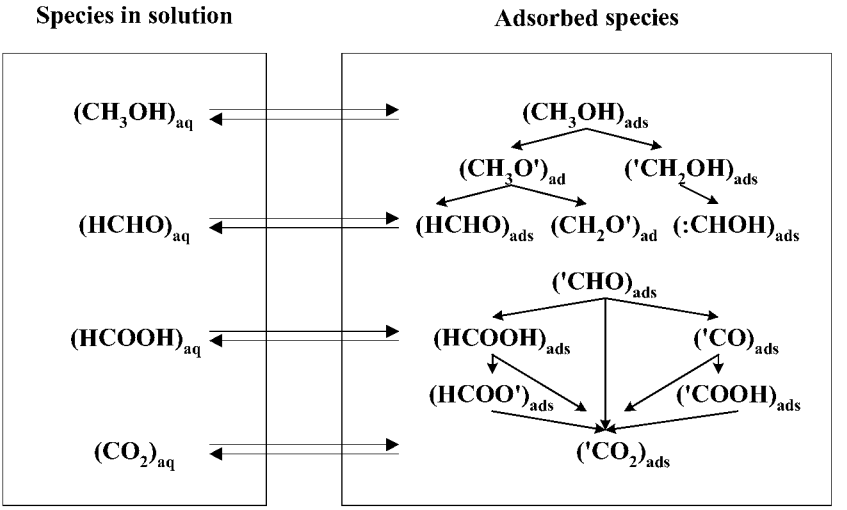

Figure 2.9. Various possible pathways for the electrooxidation of methanol.

acid in parallel reactions.[2] These, in turn, could then be oxidized to methanol. Such possible reaction pathways for methanol oxidation[18] are represented in Figure 2.9.

2.4. CONCEPT OF RATE-DETERMINING STEP

The term *rate-determining step* (rds) is frequently referred to the step in reactions that proceed in two or more intermediate stages, either consecutively or in parallel. Most often, it is only one of these intermediate steps, which controls the rate of the overall reaction; this step is given the terminology *the rate-determining step* or *rds*. Several analogies have been proposed to visualize the concept of the rds in a consecutive reaction. One is that of an electrical circuit with a series of two or more resistances and a power source, as shown in Figure 2.10. This figure shows three resistors, R_1, R_2, and R_3 in series; in addition, the power source (a fuel cell or a battery) has an internal resistance, R_i. The current (I) through the electrical circuit is given by the expression:

$$I = \frac{E}{R_1 + R_2 + R_3 + R_i} \tag{2.35}$$

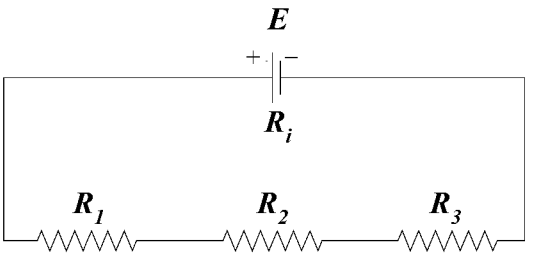

Figure 2.10. Electrical analogy for a rate-determining step in a consecutive reaction. Reprinted from J. O'M Bockris and S. Srinivasan, *Fuel Cells: Their Electrochemistry*, Copyright © 1969, with permission from McGraw-Hill Book Company.

[2] It must be noted that the proton in the intermediate steps of oxygen reduction (Eqs. 2.30 to 2.33) and in the overall reaction (Eq. 2.34) is designated as H_3O : the bare proton does not exist as such in an aqueous medium. Due to the charge on the proton, its size and the strong ion-dipole reaction with the H_2O molecule, it forms the hydronium ion, H_3O , which is the discharging entity. The dissociation energy for breaking this bond is 183 kJ mol^{-1}.

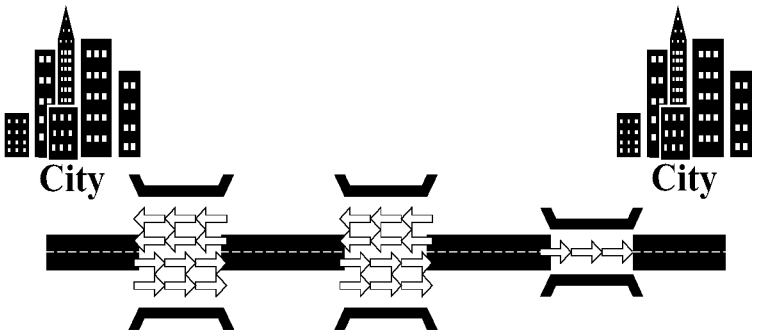

Figure 2.11. Roadblock analog for the rate-determining step in a consecutive reaction. Reprinted from J. O'M Bockris and S. Srinivasan, *Fuel Cells: Their Electrochemistry*, Copyright © 1969, with permission from McGraw-Hill Book Company.

where E is the electric potential of the power source. Assuming that the resistances R_1, R_3, and R_i are very small in comparison to the resistance R_2, the current in the electrical circuit may be expressed by the equation:

$$I = \frac{E}{R_2} \tag{2.36}$$

which means that the resistor R_2 determines the current through the external circuit, and it is the *current-determining resistor.*

Another analogy is that of a roadblock between two cities, A & B, as represented by Figure 2.11. If one imagines several bridges between the cities, the flow of traffic in both directions will be quite fast but if there is one bridge which will let only one car travel on the bridge at a time, the speed of this car through the bridge will have a significant effect on the time for travel between the two cities.

Transforming these analogies to that of a consecutive reaction with about five intermediate steps, one can show from a plot of the free energy vs. distance along a reaction coordinate, that the step exhibiting the highest energy state with respect to the initial or final state controls the rate of the reaction. An analytical treatment of consecutive reactions carried out by Christiansen,[19] has shown that the rate-determining step controls the rate of the consecutive reaction in the forward and reverse direction, and that all other steps are virtually in equilibrium. Thus, for the chemical reaction represented in Figure 2.12, the rate of the forward reaction is given by:

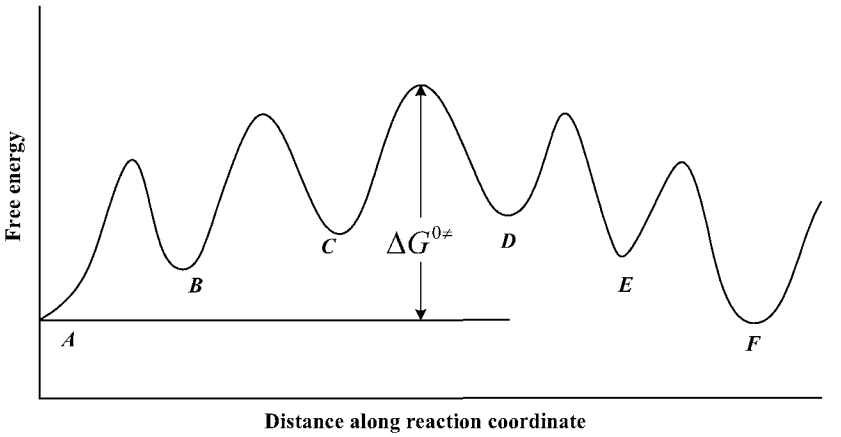

Figure 2.12. A typical free energy vs. distance along reaction coordinate plot for a consecutive reaction. Reprinted from J. O'M Bockris and S. Srinivasan, *Fuel Cells: Their Electrochemistry*, Copyright © 1969, with permission from McGraw-Hill Book Company.

$$\vec{v} = k_{C \to D}[C] \tag{2.37}$$

The rate-determining step has the highest barrier with respect to the initial or final state. It must be pointed out that according to the classical mechanical

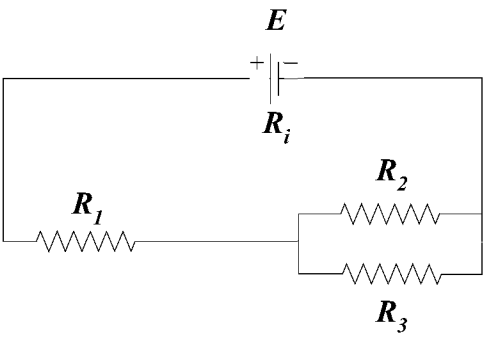

Figure 2.13. Electrical analogue for rate-determining step in a parallel reaction. Reprinted from J. O'M Bockris and S. Srinivasan, *Fuel Cells: Their Electrochemistry*, Copyright © 1969, with permission from McGraw-Hill Book Company.

treatment of reaction rates, it is only the reactant particles with sufficient energy to surmount the barriers from A to D for the forward reaction and F to C for the reverse reaction that are effective for the occurrences of the forward and reverse reactions. By using a Maxwell-Boltzmann statistical analysis, the rate of the reaction will be the same as expressed by Eq. (2.37) for the forward reaction.

In the case of a parallel reaction too, the electrical and roadblock analogs are helpful at understanding the rate-determining step. From Figure 2.13 for the former case, the current (I) in the external circuit is given by:

$$I = \frac{E}{R_1 + \dfrac{R_2 R_3}{R_2 + R_3} + R_i} \tag{2.38}$$

Assuming that R_i and R_1 are much less than R_2 or R_3 and that $R_2 << R_3$, I will approximate to

$$I \approx \frac{E}{R_2} \tag{2.39}$$

Thus, in a parallel circuit, the smaller resistor controls the current.

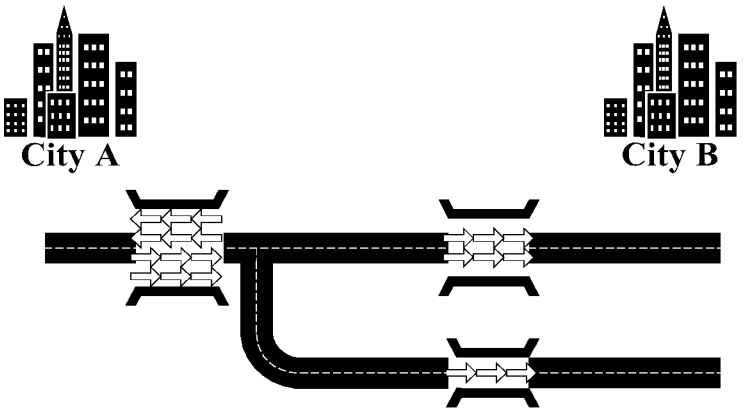

Figure 2.14. Roadblock analog for rate-determining step in a parallel reaction. Reprinted from J. O'M Bockris and S. Srinivasan, *Fuel Cells: Their Electrochemistry*, Copyright © 1969, with permission from McGraw-Hill Book Company.

For the roadblock analogy (Figure 2.14), the parallel road, which is considerably wider, determines the rate of the cars travelling between the cities A and B.

In terms of a chemical reaction, one may consider the sequence:

$$A \underset{v_{-1}}{\overset{v_1}{\rightleftarrows}} B \overset{v_2}{\rightarrow} C_1 \quad B \overset{v_{-2}}{\rightarrow} C_2 \tag{2.40}$$

For simplicity, the rates (v) of the intermediate steps C_1 to B and C_2 to B may be considered negligible. Thus,

$$v_1 - v_{-1} = v_2 + v_3 \tag{2.41}$$

If

$$v_2 >> v_3 \tag{2.42}$$

then

$$v_1 - v_{-1} \approx v_2 \tag{2.43}$$

Further if

$$v_1 >> v_2 \tag{2.44}$$

then,

$$v_1 \approx v_{-1} \tag{2.45}$$

Thus, the step A $\rightarrow$ B is virtually in equilibrium and the step B $\rightarrow$ C controls the rate of the overall reaction.

Another possible type of consecutive reaction is one with a *dual* or *coupled mechanism*. In such a case, the standard free energies of the activated complexes in two steps of a consecutive reaction could be nearly the same, and the forward velocities of the two steps will be identical. These two steps control the rate of the overall dual reaction. A consecutive reaction in which the velocities of the two reverse steps are negligible in comparison with the forward rates is referred to as a *coupled reaction*.

2.5. DEPENDENCE OF CURRENT DENSITY ON POTENTIAL FOR ACTIVATION-CONTROLLED REACTIONS: THEORETICAL ANALYSIS

2.5.1. Classical Treatment to Determine Electrode Kinetic Parameters

In electrochemical reactions, the potential across the interface affects the rate of the reaction. The reason is that in an electrochemical reaction an electron transfer reaction occurs across the interface, and the rate of this reaction could be significantly affected by the electric field across the double layer at the interface.

Let us first consider a chemical reaction such as:

$$A + B \rightarrow [AB]^{\ddagger} \rightarrow C + D \tag{2.46}$$

where A and B are the reactants, C and D the products, and $[AB]^{\ddagger}$ represents the activated state for the reaction. Assuming that this reaction occurs in a single step and that the potential energy for the reaction is represented as a function of the reaction coordinate (Figure 2.15), the velocity of the reaction (v) may be expressed by:

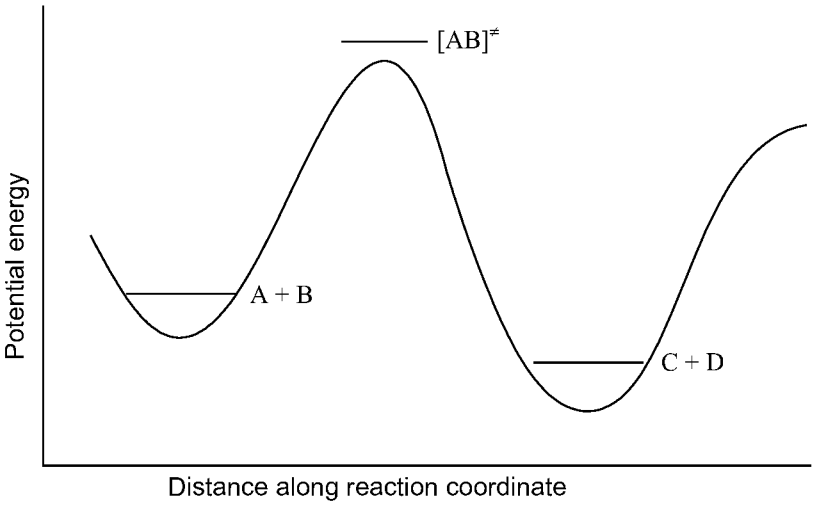

Figure 2.15. Potential energy profile along the reaction path for a single step reaction. Reprinted from J. O'M Bockris and S. Srinivasan, *Fuel Cells: Their Electrochemistry*, Copyright © 1969, with permission from McGraw-Hill Book Company.

$$v = \frac{kT}{h}[\mathrm{A}][\mathrm{B}]\exp\left(-\frac{\Delta H^{O\ddagger}}{RT}\right)\exp\left(\frac{\Delta S^{0\ddagger}}{R}\right) \tag{2.47}$$

where $\Delta H^{0\ddagger}$ and $\Delta S^{0\ddagger}$ are the enthalpies and entropies for activation. The rate constant for this reaction, k_0, is thus:

$$k_0 = \frac{kT}{h}\exp\left(-\frac{\Delta H^{0\ddagger}}{RT}\right)\exp\left(\frac{\Delta S^{0\ddagger}}{R}\right) \tag{2.48}$$

Only a simplified version of the chemical kinetics is presented above for the case of a single-step reaction. The calculations of potential energy versus reaction coordinate are much more complex and sophisticated for multi-step reactions because if more than three atoms are involved, there is an increase in the number of interaction energies to be considered in the potential energy calculations. Statistical mechanical treatments, involving calculations of the translational, rotational, and vibrational partition functions for the activated and initial states, have been made.

However, conceptually it is possible to arrive at a general expression, such as Eq. (2.47) for the rate of a reaction occurring in consecutive steps. The rate constants for the forward, $\vec{k}$, and reverse, $\overleftarrow{k}$, reactions can then be modified to:

$$\vec{k} = \frac{kT}{h}\exp\left(-\frac{\Delta G^{0\ddagger}_{i\to g}}{RT}\right) \tag{2.49}$$

and

$$\overleftarrow{k} = \frac{kT}{h}\exp\left(-\frac{\Delta G^{0\ddagger}_{n\to g}}{RT}\right) \tag{2.50}$$

for a reaction which occurs in n steps with the g^{th} step being the rate-controlling step. Similar treatments have been carried out for multistep reactions that occur by parallel-reaction paths or by dual or coupled mechanisms. For more details, the reader is referred to textbooks on the kinetics of chemical reactions.

The above description can now be extended to electrochemical reactions such as:

$$\mathrm{M} + \mathrm{AB}^{+} + \mathrm{e}_0^{-} \rightarrow \mathrm{MA} + \mathrm{B} \tag{2.51}$$

An example of this reaction is proton discharge during hydrogen evolution, e.g.,

$$M + H_3O^+ + e_0^- \rightarrow MH + H_2O \quad (2.52)$$

For this case, a potential energy profile (Figure 2.16) can be constructed by assuming that in the initial state a strong H^+-H_2O bond stretches as this species comes towards the metal surface and an M-H bond formation (chemisorption of hydrogen) starts to occur, as represented by:

$$M + H^+ \cdots H_2O + e_0^- \rightarrow [M \cdots H^+ \cdots H_2O] + e_0^- \rightarrow MH + H_2O \quad (2.53)$$

Butler first proposed that the transfer of the electron from a stretched H^+-H_2O to a stretched M – H bond occurs at the activated state via a tunnelling mechanism.[20] When an electric field is applied across the interface, it affects the potential energy profile for the stretching of the H^+-H_2O bond plus the electron but not for the final state, MH_x. It must be noted that the electric energy across the interface varies linearly with distance. The net result is that the potential energy vs.

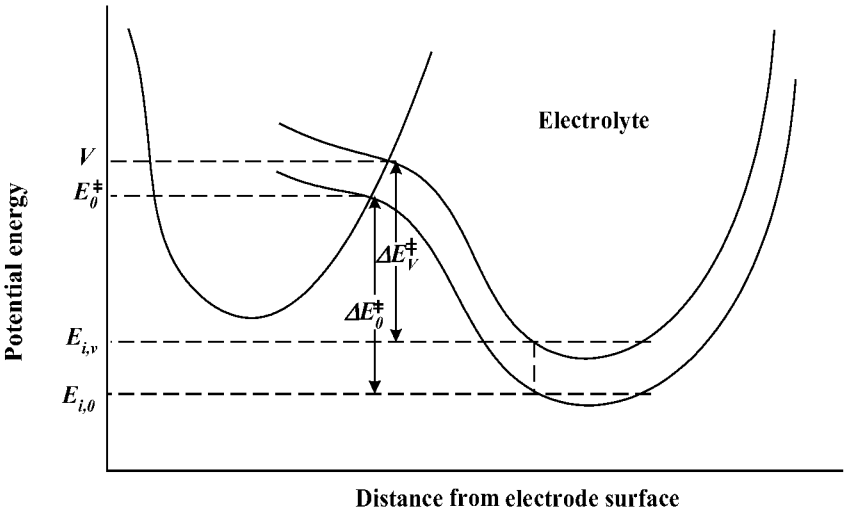

Figure 2.16. Potential energy vs. distance along reaction coordinate plot for transfer of proton from H^+–H_2O to metal forming the adsorbed M–H bond as an intermediate during hydrogen evolution. $E_{i,0}$ and $E_{i,V}$ represent the zero point energy levels of the initial state H^+–H_2O when the potentials across the metal/electrolyte interface are V = 0 and $V = V$, respectively; $\Delta E_0^{\ddagger}$ and $\Delta E_V^{\ddagger}$ and are the corresponding energies for the activated state; and $E_0^{\ddagger}$ and $E_V^{\ddagger}$ are the corresponding activation energies for the reaction. Reprinted from J. O'M Bockris and S. Srinivasan, *Fuel Cells: Their Electrochemistry*, Copyright © 1969, with permission from McGraw-Hill Book Company.

distance plot for the stretching of the initial state is raised effectively by a value of VF for the initial state, where V represents the potential across the interface. In the activated state, the effect of the field is only a fraction of that of the initial state. Thus, the rate constant for the proton discharge step (k) can be given by an equation of the form:

$$k = k_0 \exp\left(-\frac{\beta VF}{RT}\right) \tag{2.54}$$

where k_0 denotes the value of the rate constant when there is no electric field across the interface (i.e., $V = 0$); β is referred to as the *symmetry factor*, and it represents a fraction of the field which changes the potential energy of the activated state when there is a potential of V volts across the interface. It must be stressed that a simplified version is presented here, and for more rigorous treatments, the reader is referred to books on electrochemistry.

Just as in chemical kinetics, the next step is to obtain an expression for the *velocity* or *rate* of electrochemical reactions, which will depend on the kinetic parameters such as the concentration of the reactants, reaction order etc. The rate of an electrochemical reaction at an electrode/electrolyte interface is expressed as a current density (A or mA cm^{-2}) and is measured at constant temperature. Determination of the manner in which the current density is dependent on the potential is one of the most important diagnostic criteria in elucidating the mechanism of an electrochemical reaction, i.e., the reaction path, intermediate steps, and rate-determining step. In this chapter we present only the essential theoretical analysis for determining the mechanism of the electrochemical reactions. Chapters 5 and 6 will discuss the electrocatalytic factors involved in fuel cell reactions, and illustrate the experimental methods to (i) determine the mechanisms of the electrochemical reactions of fuel cells; and (ii) elucidate the intermediate steps and the rate-determining step, which leads to an evaluation of the electrode kinetic parameters for the reaction.

In the remainder of this section, we shall deal with the expressions for current density as a function of potential, reaction orders, and exchange current densities. A short description will also be made about stoichiometric number, which is often encountered in investigations of the kinetics of reactions via consecutive or parallel-reaction pathways.

2.5.1.1. *Expression for Current Density as a Function of Potential.* Just as in the case of a chemical reaction, the rate constant for an electrochemical reaction is given by k (Eq. 2.54) and the rate of the reaction (ν) depends on the activities of the reactants for the forward reaction and of the products for the reverse reaction. The net rate of the reaction expressed by Eq. (2.52) is given by:

$$\nu = \vec{\nu} - \overleftarrow{\nu} \tag{2.55}$$

where $\vec{v}$ and $\overleftarrow{v}$ are the rates of the forward and reverse reactions, respectively. They are expressed as

$$\vec{v} = \vec{k}_0 c_{H_3O^+} (1-\theta) \exp\left(-\frac{\beta VF}{RT}\right) \tag{2.56}$$

$$\overleftarrow{v} = \overleftarrow{k}_0 \theta \exp\left[\frac{(1-\beta)VF}{RT}\right] \tag{2.57}$$

where $c_{H_3O^+}$ is the concentration of H_3O^+ and θ is the fractional degree of coverage of the species MH at the surface of the electrode. In these equations, it is assumed that the reaction is first order with respect to the concentrations of reactants and products. The terms θ and (1 - θ) arose in the above two equations because we assumed a Langmuir adsorption for the chemisorption of MH on the electrode. The velocities of the forward and reverse reaction are in mol s^{-1} for unit area of the electrode. To convert the velocities to current densities, one has to multiply the velocity by *nF*, which represents the number of coulombs involved during the charge transfer. In the chosen reaction (Eq. 2.57), *n* is equal to unity. For the transformation of the proton plus one electron to an adsorbed hydrogen atom (MH), the current density (*i*) can then be expressed by:

$$i = \vec{i} - \overleftarrow{i} = F\left[\vec{k}_0 c_{H_3O^+} (1-\theta) \exp\left(-\frac{\beta VF}{RT}\right) - \overleftarrow{k}_0 \theta \exp\left(\frac{(1-\beta)VF}{RT}\right)\right] \tag{2.58}$$

The above expression is for the net current density for the discharge of the proton on the metal to form an adsorbed hydrogen atom on the metal. The species MH is an intermediate and not a final product. This step is then followed by one of the following intermediate steps for the overall electrolytic evolution of hydrogen:

$$2\mathrm{MH} \underset{k_{-2}}{\overset{k_2}{\rightleftharpoons}} 2\mathrm{M} + \mathrm{H_2} \tag{2.59}$$

$$\mathrm{MH} + \mathrm{H_3O^+} + \mathrm{e^-} \underset{k_{-3}}{\overset{k_3}{\rightleftharpoons}} \mathrm{M} + \mathrm{H_2} + \mathrm{H_2O} \tag{2.60}$$

for which the current density-potential relations are given by:

$$i = 2F\left[k_2\theta^2 - k_{-2}(1-\theta^2)P_{H_2}\right] \tag{2.61}$$

or

$$i = F\left[k_3 c_{H_3O^+}\theta \exp\left(-\frac{\beta VF}{RT}\right) - k_{-3}(1-\theta)P_{H_2}\exp\left(\frac{(1-\beta)VF}{RT}\right)\right] \qquad (2.62)$$

The intermediate step, as represented by Eq. (2.59), is referred to as the *recombination step,* and by Eq. (2.60) as the *electrochemical-desorption step.* It must be noted that there is no apparent potential dependence for the former but there is one for the latter. However, in the former case, there is the indirect potential dependence from the first step and a modified one for the second step because of the dependence of θ (concentration of the MH_{ads} species) on the potential.

In order to arrive at an expression of $i = f(V)$ for the overall reaction, it is necessary for one to assume (i) a reaction pathway (i.e., discharge-recombination or discharge-electrochemical desorption) and (ii) whether the first or the second step is the rate-determining step in the two consecutive pathways. These expressions are presented in Table 2.1 for both pathways and the two possible rate-determining steps for each pathway. One can also make further approximations, particularly for the Langmuir conditions of adsorption, for θ tends to zero or unity and simplify the expressions as shown in Table 2.1. Another possible pathway frequently encountered is the coupled reaction slow discharge/slow electrochemical desorption. In this case, both the discharge and the electrochemical desorption intermediate steps have equal rates.

2.5.1.2. *Reaction Orders, Transfer Coefficients, and Stoichiometric Numbers.* Just as in the case of rates of chemical reactions, the rates of electrochemical reactions depend on the activities (concentrations) of reactants and products. One frequently encounters the term *reaction order* with respect to a particular reactant. Depending on the simplicity or complexity of a reaction which may occur in a single step or multi-step and on the rate-determining step, the reaction order could be unity, zero, or greater than or less than one (whole or fractional). In general terms, for an overall electrochemical reaction of the type

$$aA + bB + ... + ne_0^- \rightarrow xX + yY + ... \qquad (2.63)$$

If the rate-determining step is

$$lL + mM + ... + n'e_0^- \rightarrow pP + qQ + ... \qquad (2.64)$$

and its velocity is given by

$$v = ka_L^l a_M^m ..... \exp\left(\frac{\alpha VF}{RT}\right) \qquad (2.65)$$

The reaction order, *l*, for the reactant, L, is given by:

$$l = \left(\frac{\partial \ln v}{\partial \ln a_L} \right)_{\alpha_M \ldots\ldots V,T} \tag{2.66}$$

In Eq. (2.65), α, the transfer coefficient, is related to the symmetry factor β; it may or may not be equal to β. The numerical value of α would depend on how many of the preceding or succeeding steps involve an electron transfer. Table 2.1 shows the reaction orders and the transfer coefficients for the different possible rate-determining steps according to the two reaction pathways for the hydrogen evolution reaction.

The *stoichiometric number*, ν, is a term used in one of the columns in Table 2.1. This term represents the number of times the rate-determining step has to take place for one act of the overall reaction. For instance, for a mechanism involving slow discharge followed by a fast recombination step, the stoichiometric number is two, but for a slow discharge followed by an electrochemical desorption step, the stoichiometric number is unity. One of the fundamental aspects of electrode kinetics is that the parameters, Tafel slopes, symmetry factors, transfer coefficients, reaction orders, stoichiometric numbers, and separation factors[3] are diagnostic criteria for determining the mechanisms of electrochemical reactions, i.e., the reaction path and the rate-determining step.

2.5.1.3. *Exchange-Current Density and Reversible Potential.* To explain the concept of exchange-current density (i_0), let us consider a single step reaction:

$$\mathrm{O} + n\mathrm{e}_0^- \rightarrow \mathrm{R} \tag{2.67}$$

where O and R are the oxidized and reduced species, respectively, in the reaction. Thus, for this reaction, the net current density, i, may be expressed by:

$$i = F\left[\vec{k}^{\,0} c_O \exp\left(-\frac{\beta V_r F}{RT} \right) - \overleftarrow{k}^{\,0} c_R \exp\left(\frac{(1-\beta) V_r F}{RT} \right) \right] \tag{2.68}$$

As represented above, the net current density is for the cathodic reduction of species O to R. Under equilibrium conditions, i.e., at the reversible potential, the net current

[3] In Table 2.1 the parameter S_T represents the hydrogen-tritium *separation factor*, defined as the ratio of hydrogen/tritium in the gas phase to the electrolyte. This parameter is also a diagnostic criteria in elucidating the mechanism of electrolytic-hydrogen evolution.

TABLE 2.1
Kinetic Parameters for the Most Probable Mechanisms of the Hydrogen Evolution Reaction[a]

	Condition $\theta \rightarrow 0$				Condition $\theta \rightarrow 1$					
Mechanism	$\frac{\partial\eta}{\partial \ln i}$	$\frac{\partial\eta}{\partial \ln a_{H_3O^+}}$	$\frac{\partial\eta}{\partial \ln p_{H_2}}$	$\frac{\partial\eta}{\partial \ln\theta}$	$\frac{\partial\eta}{\partial \ln i}$	$\frac{\partial\eta}{\partial \ln a_{H_3O^+}}$	$\frac{\partial\eta}{\partial \ln p_{H_2}}$	$\frac{\partial\eta}{\partial \ln\theta}$	ν	S_T
Slow discharge-fast recombination	$-\frac{RT}{\beta F}$	$\frac{RT}{F}$	$\frac{RT}{2F}$	0	$-\frac{RT}{\beta F}$	$\frac{RT}{F}$	$-\frac{RT}{2F}\frac{(1-\beta)}{\beta}$	0	2	5
Fast discharge-slow recombination	$-\frac{RT}{2F}$	0	$\frac{RT}{2F}$	$-\frac{RT}{F}$	∞	0		0	1	11
Coupled discharge recombination	$-\frac{RT}{\beta F}$	$\frac{RT}{F}$	$\frac{RT}{2F}$	$\frac{2RT}{\beta F}$	$-\frac{RT}{\beta F}$	$\frac{RT}{F}$	$-\frac{RT}{2F}\frac{(1-\beta)}{\beta}$	$-\infty$		5
Slow discharge-fast electrochemical desorption	$-\frac{RT}{\beta F}$	$\frac{RT}{F}$	$\frac{RT}{2F}$	$\frac{RT}{F}$	$-\frac{RT}{(1+\beta)F}$	$\frac{RT}{F}\frac{(1-\beta)}{(1+\beta)}$	$-\frac{RT}{2F}\frac{(1-\beta)}{(1+\beta)}$	0	1	6
Fast discharge-slow electrochemical desorption	$-\frac{RT}{(1+\beta)F}$	$\frac{RT}{F}\frac{(1-\beta)}{(1+\beta)}$	$\frac{RT}{2F}$	$-\frac{RT}{F}$	$-\frac{RT}{\beta F}$	$\frac{RT}{F}$	$\frac{RT}{2F}$	0	1	23
Coupled discharge-electrochemical desorption	$-\frac{RT}{\beta F}$	$\frac{RT}{F}$	$\frac{RT}{2F}$	0	$-\frac{RT}{\beta F}$	$\frac{RT}{F}$	$\frac{RT}{2F}$	0		7
Slow molecular hydrogen-ion discharge	$-\frac{RT}{(1+\beta)F}$	$\frac{RT}{F}\frac{(1-\beta)}{(1+\beta)}$	$\frac{RT}{2F}$	$-\frac{RT}{F}$	$-\frac{RT}{\beta F}$	$\frac{RT}{F}$	$\frac{RT}{2F}$	0	1	6
Slow molecular hydrogen diffusion	$-\frac{RT}{2F}$	0		$-\frac{RT}{F}$	∞	0		0	1	8

[a] From Suggested Reading 1.

density is zero. The *exchange-current density* (i_0) may be defined as the rate of the forward or reverse reaction under equilibrium conditions. Thus,

$$i_0 = \vec{i} - \overleftarrow{i} = 0 \tag{2.69}$$

and

$$i_0 \equiv \vec{i} = \overleftarrow{i} = F\vec{k}^{\,0} c_O \exp\frac{-\beta V_r F}{RT} = F\overleftarrow{k}^{\,0} c_R \exp\frac{(1-\beta)V_r F}{RT} \tag{2.70}$$

From Eq. (2.70), it follows that an expression for V_r, the *reversible potential*, is:

$$V_r = \frac{RT}{F}\ln\frac{\vec{k}^{\,0}}{\overleftarrow{k}^{\,0}} + \frac{RT}{F}\ln\frac{c_O}{c_R} \tag{2.71}$$

This equation for the half-cell reaction is exactly the same as for the Nernst reversible potential, which was derived in Section 1.5. The first term on the right hand side represents the standard reversible potential for conditions of unit activities of reactants and products and the temperature is assumed to be 25 ^{0}C. The second term reflects the change in the reversible potential with the change in concentrations of reactants and products. The expressions are similar for more complex reactions involving more than one reactant and one product and for multi-electron transfer reactions, which occur in consecutive or parallel steps but the formats for i_0 and V_r are similar. In general terms, for the reaction expressed by Eq. (2.64), these could be expressed by:

$$i_0 = \vec{i} = \overleftarrow{i} = F\vec{k}^{\,0} c_O \exp\left(-\frac{\beta V_r F}{RT}\right) = F\overleftarrow{k}^{\,0} c_R \exp\left(\frac{(1-\beta)V_r F}{RT}\right) \tag{2.72}$$

From Eq. (2.72), the expression for V_r, the reversible potential, is:

$$V_r = \frac{RT}{F}\ln\left(\frac{\vec{k}^{\,0}}{\overleftarrow{k}^{\,0}}\right) + \frac{RT}{F}\ln\left(\frac{c_O}{c_R}\right) \tag{2.73}$$

2.5.2. Quantum Mechanical Treatment

In the preceding section, a classical kinetic treatment was followed to derive the expression for the rate of a charge-transfer reaction, i.e., the first step of proton discharge on the electrode surface to form an adsorbed hydrogen atom on the metal;

this step is then followed by the recombination or electrochemical desorption step in the overall hydrogen evolution reaction (see Eqs. 2.52, 2.59, and 2.60). In such a treatment, it is assumed that the reactants, which have sufficient kinetic energy (i.e., greater than the potential energy barrier), can proceed at a rate dependent on (i) kT/h, (ii) the product of reactant concentrations, and (iii) the free energy of activation. It was also assumed that the proton discharge step involves the stretching of the H^+-H_2O bond and that it occurs, only when the bonds are stretched to the intersection of the two Morse curves for the H^+-H_2O and M-H bonds. Another assumption was that the electron transfer occurs when the proton is stretched to the intersection point of the two Morse curves (Figure 2.16). Though the latter assumption is correct, it is only a quantum-mechanical treatment of electron transfer that can provide an explanation for the considerably higher rates for the proton discharge step than that predicted according to the classical treatment. It is also necessary to present another plot (Figure 2.17) for this derivation, i.e., the potential energy vs. distance plot for the transfer of an electron from the metal to the solvated proton.

According to Gurney,[21] the energy barrier for electron transfer is obtained by taking into consideration: (i) the *image interaction* given by $e^2/4x$, where e is the

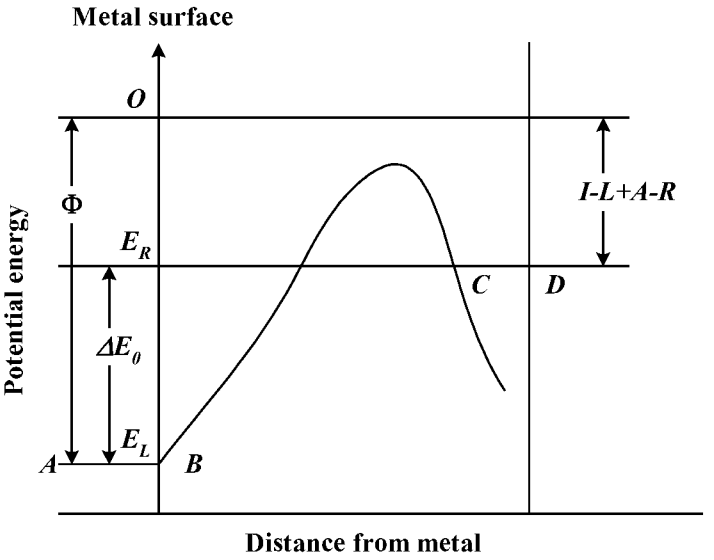

Figure 2.17. Potential energy vs. distance from the surface of the metal electrode for transfer of electron from H_3O^+ to metal. Reprinted from J. O'M Bockris and S. Srinivasan, *Fuel Cells: Their Electrochemistry*, Copyright © 1969, with permission from McGraw-Hill Book Company.

electronic charge and x is the distance of the electron from the metal surface and (ii) *the coulombic interaction* between the electron and the solvated proton. The level AB (cf. Figure 2.17) in the potential energy plot is determined by the *work function* of the metal, φ, defined as the work done in bringing an electron from an infinite distance, in vacuum, to the metal. The level CD is the work done in bringing an electron from infinity to the solvated proton. This process involves (i) the desolvation of the ion H_3O^+, (ii) the electron acceptance, (iii) formation of the M-H bond, and (iv) a repulsion between the adsorbed hydrogen atom and water molecules. The energy levels at AB (E_L) and CD (E_R) may be expressed by:

$$E_L = -\varphi \tag{2.74}$$

$$E_R = -(I - L + A - R) \tag{2.75}$$

where I is the ionization energy of the hydrogen atom, L is the interaction energy between the protons and solvent molecules with the proton at the assumed distance from the metal, A is the adsorption energy between the hydrogen atom and the metal for the specified distance, and R is the repulsion energy between the hydrogen atom and water molecule to which the proton was attached as H_3O^+, prior to charge transfer.

Numerical calculations show that according to the classical treatment, the activation energy for the transfer of electrons from the metal to the protons in solution is too high and the observed current densities cannot be explained. The only other possibility is the tunneling of electrons from the metal to the protons in solution. One of the conditions for the tunneling of the electrons from the Fermi level of the metal to the protons in solution is that there must be vacant levels in the solvated protons with energy equal to that of the former. E_L and E_R (horizontal lines) in Figure 2.17 represent the *ground states* (initial states) of the electron in the metal and the protons in the OHP. Tunneling of electrons can occur only when:

$$E_L \geq E_R \tag{2.76}$$

Using Eqs. (2.74) and (2.75) this condition becomes:

$$\varphi \leq I - L + A - R \tag{2.77}$$

The parameter I is a constant but the parameters R, A, and L are not. They depend on the distances of the hydrogen atom and ion from the metal. The potential energy curves for the stretching of the proton from its equilibrium position in the OHP and the hydrogen atom from the metal are shown in Figure 2.16. As first proposed by Butler, the only way of reducing the energy gap for electron transfer to occur is by stretching the H^+–OH_2 bond. Figure 2.16 shows that this gap is reduced to zero at the intersection point of the potential energy distance plots for the stretching of the

H^+–OH_2 bond and M–H bonds. It also shows that only a fraction of the energy (represented by LN) is required to bring the proton up to the intersection point. It must be noted that *electron tunneling* can occur left of the intersection point for stretching of the H^+–OH_2 bond but not to its right. The *discharge step* may then be represented by:

$$H_3O^+ + M(e^-_0) \rightarrow \left[H_2O - H^+ + M(e^-_0)\right]^{\neq} \underset{\leftarrow}{\rightarrow} [H_2O + H - M]^{\neq} \rightarrow H_2O + H - M \tag{2.78}$$

The potential energy plot in Figure 2.17 is illustrated for the case when the potential drop across the electrode/electrolyte interface is zero. When the potential drop is V, as applied in the cathodic direction for speeding up the reaction,

$$\Delta E_V = \Delta E_0 + VF \tag{2.79}$$

where ΔE_V and ΔE_0 are the energies at the potentials V and zero, respectively. It must be noted that V has a negative value for the cathodic direction. Since

$$\Delta E_0^{\neq} = \beta \Delta E_0 \quad \text{and} \quad \Delta E_V^{\neq} = \beta \Delta E_V \tag{2.80}$$

it also follows from the two preceding equations that

$$\Delta E_V^{\neq} = \beta(\Delta E_0 + VF) \tag{2.81}$$

where β, the symmetry factor, represents the fraction of the energy gap between AB and CD to close the gap for electron tunneling.

The electron transfer rapidly occurs when the proton is stretched up to the intersection point of the two Morse curves (Figure 2.16). When the electrode/electrolyte potential is zero, the rate of the overall hydrogen-evolution reaction may be expressed by

$$i_V = e k_{ef} W(E_f)(W\Delta E^{\neq}) n_{H_3O^+} \tag{2.82}$$

where e is the electronic charge, k_{ef} is the *frequency factor* (number of electrons with Fermi energy, colliding with the unit area of the surface at the electrode/electrolyte interface, $W(E_f)$ is the probability of the electron being able to tunnel through the barrier, $(W\Delta E^{\neq})$ is the probability that an H_3O^+ is in a suitably stretched state for electron transfer to occur, and $n_{H_3O^+}$ is the number of H_3O^+ ions populating the unit area of the OHP. Approximate expressions for k_{ef} and $W(E_f)$ are:

$$k_{ef} = \frac{4\pi m(kT)^2}{h^3} \tag{2.83}$$

and

$$W_{ef} = \exp -\frac{4\pi l}{h}\left[2m\left(E_x - E_f\right)^{1/2}\right] \tag{2.84}$$

where m is the mass of the electron, E_x is the energy at the top of the electron transfer barrier, and l is the width of the barrier (the barrier is assumed to be rectangular). For $(W\Delta E_0^{\neq})$, a Boltzman expression may be used, i.e.,

$$(W\Delta E_0^{\neq}) = \exp\frac{-\Delta E_0^{\neq}}{kT} \tag{2.85}$$

Substituting Eqs. (2.83) to (2.85) in Eq. (2.82),

$$i_{V=0} = 4\pi em\frac{(kT)^2}{h^3}\exp\left[-\frac{4\pi l(2m)}{h}\left(E_x - E_F\right)^{1/2}\right]\exp\left(\frac{-\Delta E_0^{\neq}}{kT}\right)n_{H_3O^+} \tag{2.86}$$

The main difference in the above expression for the current density at a potential V will be that ΔE_0 in the last term is replaced by ΔE_V. From Eqs. (2.80) and (2.81), it follows that,

$$\Delta E_V^{\neq} - \Delta E_0^{\neq} = \beta VF \tag{2.87}$$

Thus, at a potential V, Eq. (2.86) is transformed to:

$$i_{V=V} = i_{V=0}\exp(-\frac{\beta VF}{RT}) \tag{2.88}$$

By using $V = V_r + \eta$, where η is the *activation overpotential* and $V = V_r$ for the reversible potential at which i - i_0, one arrives at the equation:

$$i = i_0\ \exp(-\frac{\beta\eta F}{RT}) \tag{2.89}$$

which is the empirical Tafel equation that was also arrived at following the classical treatment. The main difference between the classical and quantum mechanical treatments is that the calculations yield reasonable values of the exchange current

density, consistent with the experimental ones in the former case but would yield considerably lower values in the latter case.

Section 1.3 dealt with several types of electrochemical reactions. The charge transfer steps in practically all these types of reactions play key roles in determining the rates of the overall reactions. In the case of electrocatalytic reactions such as in fuel cells, water electrolysis, electroorganic oxidation and reactions, intermediate chemical steps of adsorption/desorption can also be slow enough to contribute to activation overpotentials.

2.6. CONCEPT OF ACTIVATION OVERPOTENTIAL, EXPRESSION FOR CURRENT DENSITY AS A FUNCTION OF ACTIVATION OVERPOTENTIAL, AND CHARGE TRANSFER RESISTANCE

To express the current density-potential relations in simpler terms, another term deserves a definition, i.e., the *overpotential,* η, for the reaction. The *activation overpotential* (η), for a reaction controlled by charge transfer in an electrochemical reaction, is the extent of departure of the potential, across the electrode/electrolyte interface (at which this reaction occurs), from the reversible potential, when the reaction occurs at a net current density of i A cm^{-2}. The *overpotential*, like *overheat* for a chemical reaction, is the driving force for the electrochemical reaction. For a cathodic reaction (as the one represented by Eq. 2.67) the overpotential is negative, and for an anodic reaction, it is positive. For the reaction expressed by Eq. (2.67), one can transform Eq. (2.68) into the form:

$$i = i_0\left[\exp\left(-\frac{\beta\eta F}{RT}\right) - \exp\left(\frac{(1-\beta)\eta F}{RT}\right)\right] \tag{2.90}$$

using the equation

$$V = V_r + \eta \tag{2.91}$$

and the expressions for i_0 are given by Eqs. (2.69) and (2.70).

In more general terms, the familiar form of the equation for a multistep reaction involves α, the *transfer coefficient*, instead of β, the symmetry factor, which is valid for a single-step reaction. Thus, in general terms,

$$i = i_0\left\{\exp\left[-\frac{\alpha\eta F}{RT}\right] - \exp\left[\frac{(1-\alpha)\eta F}{RT}\right]\right\} \tag{2.92}$$

Two limiting cases can now be considered. One is at a low overpotential, when the exponential terms in Equation (2.92) can be linearized. This applies at less than 20 mV at room temperature. For such a case, this equation becomes:

$$i = \frac{i_0 \eta F}{RT} \tag{2.93}$$

Thus, at potentials close to the reversible potential for the reaction, there is a linear dependence of current density on overpotential. Considering an electrical analog, one may introduce the term *charge transfer resistance* (R_{ct}) for the electrochemical reaction in this linear region, which is defined as:

$$R_{ct} = \frac{d\eta}{di} = \frac{RT}{i_0 F} \tag{2.94}$$

From this equation, it is clear that if the exchange current density, i_0, has low values for the charge-transfer reaction, the charge transfer resistance is high and vice versa. The term *highly polarizable* and *pseudo-nonpolarizable* reactions are often used for such cases. The former is for irreversible reactions and the latter is for pseudo-reversible reactions. For highly reversible reactions, $i_0 \geq 10^{-3}$ A cm^{-2} (e.g., hydrogen evolution/ionization on platinum electrodes in acid media, copper deposition/dissolution) and for highly irreversible reactions, generally $i_0 \leq 10^{-6}$ A cm^{-2} (e.g., oxygen evolution/reduction, methanol oxidation).

The other limiting case occurs when η exceeds about 20 or more mV. Under these conditions, the current density for the reverse reaction is small in comparison with the forward reaction. Thus, the expression for the current density as a function of overpotential reduces from Equation (2.92) to

$$i = i_0 \exp\left(-\frac{\alpha \eta F}{RT}\right) \tag{2.95}$$

which may be written in the form

$$\eta = \frac{RT}{\alpha F} \ln i_0 - \frac{RT}{\alpha F} \ln i \tag{2.96}$$

This is identical with the equation:

$$\eta = a + b \ln i \tag{2.97}$$

empirically proposed by Tafel in 1905. The parameters a and b are the Tafel parameters. According to this equation, there is a semi-logarithmic dependence of the overpotential on the current density. In the Tafel region, the charge transfer resistance (R_{ct}) is given by

$$R_{ct} = \frac{d\eta}{di} = \frac{b}{i} \tag{2.98}$$

Thus, in this region R_{ct} decreases inversely with i. Alternatively stated, there is a semi-exponential increase of η with an increase of i for a cathodic reaction.

Quite often in electrochemical reactions, the first electron transfer step is rate determining and the value of α is then equal to the value of β (about 0.5). Thus, a Tafel slope of 120 mV decade^{-1} is frequently encountered. However, there are several cases where the second, third, and in some cases, subsequent steps are rate determining and these will generally have higher values of the transfer coefficients and correspondingly lower Tafel slopes, i.e., 60 mV, 30 mV, and 15 mV decade^{-1}. More detailed interpretations of the Tafel slopes for multi-step fuel cell reactions are presented in the Chapter 5 on *Electrocatalysis of Fuel Cell Reactions*, as well as in several books on electrode kinetics.

2.7. OTHER TYPES OF RATE LIMITATIONS AND OVERPOTENTIALS AND THEIR EFFECTS ON CURRENT DENSITY POTENTIAL BEHAVIOR

2.7.1. Mass-Transport Overpotential

So far we have focused on charge-transfer reactions that occur at interfaces of electrodes with electrolytes. The assumption was made that the transport of the reactant species to and from the OHP has no hindrances. This assumption is valid for several electrochemical reactions and for several fuel cell reactions, particularly at low to intermediate current densities. However, when the concentrations of reactants are low, particularly for gases with very low solubility in the electrolyte (for example hydrogen or oxygen), limitations occur due to the slowness of transport of these species from the bulk to the OHP where the charge transfer occurs. One type of transport limitation for the example chosen is the *diffusion* of the reactant species to the electrode surface, if ionic species are involved. There is an effect of the electric field on the rate of transport of the ionic species toward or away from the electrode. Additionally, limitations due to *convective* transport could be caused by differences in densities as a result of temperature or concentration. One can overcome most limitations caused by *migration* or convection by using supporting electrolytes in the former case and by working in still solutions in the latter. Under such conditions, diffusion alone governs mass transport. Diffusion in electrochemistry is analogous to heat transfer in solid, liquid, or gas media.

The current density–overpotential relation for an electrochemical reaction, which is controlled by the rate of diffusion of a reactant species from the bulk electrolyte to the interface, is shown below. We shall consider a reaction:

$$M^{n+} + ne_0^- \rightarrow M \tag{2.99}$$

which occurs at a planar electrode. We shall also assume that the kinetics of the reaction is determined by the rate of one-dimensional diffusion of the reactant M^{n+} to the electrode, as represented by the equation:

$$M_b^{n+} \rightarrow M_e^{n+} \tag{2.100}$$

The suffixes *b* and *e* denote the bulk and electrode-electrolyte interface where the charge-transfer reaction occurs. According to the theory of mass transport, Fick's first law expresses the *diffusion flux*, Q, as

$$Q = -D\frac{dc}{dx} \tag{2.101}$$

In order to evaluate the concentration gradient, Nernst and Merriam[22] introduced the concept of a *diffusion layer* near the electrode across which the concentration of the reactant species varies linearly with distance. It was further assumed that the concentration maintains the bulk value from the diffusion layer to the bulk of the electrolyte. There is sufficient experimental evidence to show that in unstirred electrolytes the thickness of the diffusion layer is about 5 x 10^{-2} cm. Using the Nernst-Merrium model, Eq. (2.101) for the diffusional flux will be modified as:

$$Q = -D\left(\frac{dc}{dx}\right)_{x=0} = D\frac{c_b - c_e}{\delta} \tag{2.102}$$

Under steady state conditions, the diffusional flux will be equal to the rate of the charge transfer of the reaction. Since Q is in mol cm^{-2} and n electrons are consumed in the charge-transfer reaction, the current density for the reaction under diffusion control becomes:

$$i = DnF\frac{c_b - c_e}{\delta} \tag{2.103}$$

It must be noted that the unit for D is $cm^2\ s^{-1}$. With an increase of current density, the concentration gradient across the diffusion layer becomes steeper and the maximum gradient occurs when the steady state concentration at the electrode reaches zero. Under such conditions, all the M^{n+} ions reaching the electrode undergo the charge-transfer reaction. The expression for the *limiting current density*, i_L, is, then,

$$i_L = \frac{DnFc_b}{\delta} \tag{2.104}$$

Using Eqs. (2.103) and (2.104), one may express the current density as a function of i_L, c_e, and c_b as follows:

$$i = i_L\left(1-\frac{c_e}{c_b}\right) \tag{2.105}$$

To express the current density as a function of potential for the diffusion-controlled reaction, one must make the assumption that the charge-transfer reaction is fast, i.e., quasi-reversible or virtually in equilibrium. Under these conditions, one can use the Nernst equation for the potential at the electrode/electrolyte interface (V). When $i = 0$, the concentration of the reactant M^{n+} at the electrode is the same as in the bulk (c_b). Thus,

$$V_{i=0} = V_r{}^0 + \frac{RT}{nF}\ln c_b \tag{2.106}$$

where V_r^0 is the reversible potential of the electrode. At a current density of i, the concentration at the electrode is c_e. Thus,

$$V_{i=i} = V_r{}^0 + \frac{RT}{nF}\ln c_e \tag{2.107}$$

The suffixes $i = 0$ and $i = i$ for V denote the potential of the electrode during equilibrium conditions and the passage of current density i, for each electrochemical reaction, respectively. We may now introduce the concept of *diffusion overpotential,* η_D, as given by:

$$\eta_D = V_{i=i} - V_{i=0} = \frac{RT}{nF}\ln\frac{c_e}{c_b} \tag{2.108}$$

Substituting Eqs. (2.106) to (2.108) into Eq. (2.105), we arrive at the current density–overpotential relation for the diffusion-controlled reaction:

$$i = i_L\left(1-\exp\frac{n\eta_D F}{RT}\right) \tag{2.109}$$

When η_D is small (< 20 mV), the exponential term can be linearized and the expression for i as a function of η_D reduces to:

$$i = -\left(\frac{i_L\eta_D F}{RT}\right) \tag{2.110}$$

The reason there is a negative sign on the right hand side of Eq. (2.110) is that the electrochemical reaction is a cathodic one and η_D has negative values.

A typical plot of potential vs. current density for a diffusion-controlled reaction is represented in Figure 2.18. AB corresponds to activation overpotentials; BC is the linear region representing ohmic overpotentials; CD is the region of limiting current density. At D, other electrochemical reactions with more negative reversible potentials take place as shown by region DE. The values of the diffusion coefficients for most species undergoing electrochemical reactions in aqueous media are of the order of 10^{-5} cm^2 s^{-1} at room temperature.

The range of values of the solubilities of the reactant species is very high. However, for fuel cell reactants such as hydrogen, oxygen, and several other gases, the solubility at room temperature is only of the order of 10^{-4} moles dm^{-3}. Using these values in Eq. (2.105), the limiting current densities for the electrooxidation of hydrogen or for the electroreduction of oxygen (fuel cell reactions in aqueous media), at planar electrodes, will be only about 10^{-4} A cm^{-2}. For this reason, three-dimensional porous gas diffusion electrodes are used in fuel cells to enhance the three-dimensional reaction zone and the diffusion of the reactant species to the electroactive sites by radial diffusion. In this case, for diffusion in fine pores or to spherical particles, i_L is expressed by $DnFc/r$ where r is the radius of the fine pore or the particle. In micropores or with nanoparticles, i_L can be significantly increased.

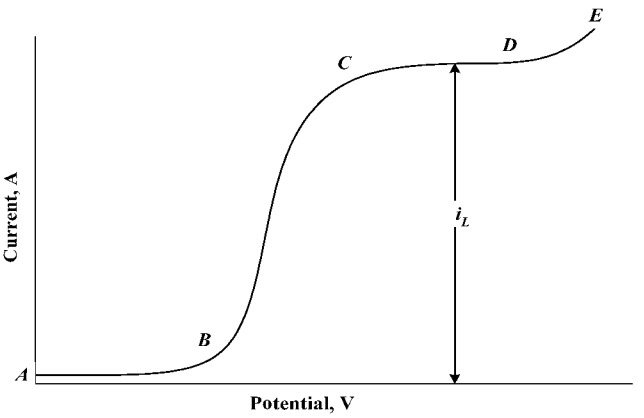

Figure 2.18. A typical plot of potential vs. current density for a diffusion-controlled reaction. Reprinted from J. O'M Bockris and S. Srinivasan, *Fuel Cells: Their Electrochemistry*, Copyright © 1969, with permission from McGraw-Hill Book Company.

2.7.2. Case of Activation plus Diffusion-Controlled Reactions

In Section 2.5, we dealt with only *activation-controlled reactions* and the preceding section dealt with a solely *diffusion-controlled reaction*. However, in real life situations, there are regions of current density where both activation and diffusion play roles, and thus, the current density-potential relation needs modification. In the case of the reaction expressed by Eq. (2.67) under conditions of solely activation control, the current density-overpotential relation is as expressed by Eq. (2.92). In arriving at this expression, one assumes that the concentrations of the reactants and products are the same at the interface and in the bulk. But at higher current densities and particularly with reactants and/or products having low solubilities, this assumption may not be valid because of the slow rate of mass transport. Under such conditions, the equation may be modified to

$$i = i_0 \left[\frac{c_{O,e}}{c_{O,b}} \exp \frac{-\beta \eta F}{RT} - \frac{c_{R,e}}{c_{R,b}} \exp \frac{(1-\beta)\eta F}{RT} \right] \tag{2.111}$$

where η is still the activation overpotential; the diffusion overpotentials are absorbed within the terms $(c_{O,e}/c_{O,b})$ and $(c_{R,e}/c_{R,b})$ (the suffixes b and e represent concentrations in the bulk and at the electrode). By taking into consideration that mixed control occurs at higher values of activation overpotentials, one can arrive at an expression without the unknown c_e terms. Since the rate of the reverse reaction is negligible, Eq. (2.111) reduces to

$$i = i_0 \frac{c_{O,e}}{c_{0,b}} \exp\left(\frac{-\beta \eta F}{RT} \right) \tag{2.112}$$

Introducing the expression for $(c_{O,e}/c_{O,b})$ from Eq. (2.106) into the above equation, one arrives at:

$$i = i_0 \left(1 - \frac{i}{i_L} \right) \exp \frac{-\beta \eta F}{RT} \tag{2.113}$$

and thus,

$$\eta = -\frac{RT}{\beta F} \ln \frac{i i_L}{i_0 (i_L - i)} \tag{2.114}$$

Another way of visualizing Eq. (2.113) is by considering the term

$$i_F = i_0 \exp\frac{-\beta\eta F}{RT} \tag{2.115}$$

where i_F is the *activation-controlled current* with no diffusional limitations. Thus, Eq. (2.114) becomes

$$\frac{1}{i} = \frac{1}{i_F} + \frac{1}{i_L} \tag{2.116}$$

The reciprocal relation provides the interpretation of an activation-diffusion controlled reaction as occurring in series and the reciprocal terms represent the charge transfer and diffusion resistances.

2.7.3. Ohmic Overpotential

Ohmic overpotential arises predominantly during the passage of an electric current and it is due to electrical resistances for the transport of ions from one electrode to the other in an electrochemical cell. The electrochemical cell is akin to an electrical circuit with a power supply and resistors in series or in parallel. In the latter case, the electrical resistance is due to transfer of electrons via the resistors. In both cases, the potential drop across the resistance (ionic in the former case and electronic in the latter) varies linearly with the amount of current passing through it. In the electrochemical case, the tip of a reference electrode (or a Luggin capillary, c.f. Chapter 6) can be placed very close to the cathode or the anode, (where the charge-transfer reaction is occurring) to record the potential with respect to the reference electrode. This half-cell potential will still include the ohmic potential drop between the test electrode and the reference electrode due to the passage of current from cathode to anode, but not the total electrolyte resistance between the anode and cathode. It was stated earlier that ohmic overpotential is predominantly due to ionic resistance. Contributions to ohmic overpotential could also be from small values of electronic resistances of the electrodes and current collectors. In the case of metallic electrodes, their electrical resistances are negligible. However, if there are passive films formed on the electrodes or if the electrodes are semiconducting materials, these could have higher electronic resistances. In order to measure the activation overpotential accurately, the ohmic resistance is measured using a *transient method* (current interrupter or ac impedance, c.f. Chapter 6). An *iR* corrected Tafel equation is of the form:

$$i = i_0 \exp\frac{\alpha F\left(\eta - \eta_{ohm}\right)}{RT} \tag{2.117}$$

where η and η_{ohm} are the measured *total* and *ohmic overpotentials*, respectively. It is assumed that there is no mass transport overpotential. The *ohmic resistance* of the electrolyte, R_{el}, can be expressed by:

$$R_{el} = \rho \frac{l}{A} \tag{2.118}$$

where ρ is the specific resistance of the electrolyte, l is the distance between the tip of the Luggin capillary (or reference) and the electrode, and A is its cross-sectional area. It must be noted that

$$\rho = \frac{1}{\kappa} \tag{2.119}$$

where κ is the specific conductivity of the electrolyte.

2.8. ELECTROCATALYSIS

2.8.1. Electrocatalysis Vital Role in Electrosynthesis and Electrochemical Energy Conversion and Storage

Electrocatalysis is an important topic in electrochemical reactions; the electrode plays a catalytic role, being the donor of electrons for the cathodic reaction or the acceptor of electrons for the anodic reaction. However, just as in heterogeneously catalyzed chemical reactions at gas/solid or at solid/liquid interfaces, the catalysts enhance steps of adsorption/desorption of intermediates. Electrocatalysis plays a significant role in electrochemical gas-evolution/gas-consumption reactions, electroorganic reactions, and bioelectrochemical reactions. Beginning in the 1920s, but more so since the 1950s, tens of thousands of publications on catalysis and electrocatalysis have appeared in the literature. Probably, the most extensively investigated electrochemical reactions are those of hydrogen and oxygen evolution (water electrolysis) and their reverse reactions (fuel cells). Electroorganic synthesis and electrooxidation of organic fuels (mostly methanol and ethanol) have also been researched but to a lesser scale. Enzymatic reactions almost always occur via electron transfer intermediate steps with the enzymes serving as electrocatalysts.

The topic of electrocatalysis is of vital importance in the investigations of fuel cell reactions, particularly the low temperature—alkaline fuel cell (AFC), proton exchange membrane fuel cell (PEMFC), direct methanol fuel cell (DMFC)—and intermediate temperature—phosphoric acid fuel cell (PAFC)—fuel cells. Even for the high temperature molten carbonate fuel cells (MCFC) and solid oxide fuel cells (SOFC), electrocatalysis has some influence on the rates of the anodic and cathodic reactions but to a considerably lesser extent than those due to ohmic and mass transport resistances. Since the early 1960s, a high percentage of the published literature is on the electrocatalysis of fuel cell reactions. In this book, Chapter 5 is devoted to the electrode kinetics and electrocatalysis of fuel cell reactions. In this chapter only summarizing remarks will be made on the topics of the distinctive and

similar characteristics in the two types of catalysis, electrocatalysis and heterogeneous catalysis.

2.8.2. Distinctive Features of Electrocatalysis

2.8.2.1. *Net-electron Transfer in Overall-Electrocatalytic Reaction.* Electrocatalysis is a field akin to heterogeneous catalysis but with one major difference: in one or more of the intermediate steps in the overall reaction, there is a net-electron transfer across the interface in electrocatalysis but not in heterogeneous catalysis. It must be noted, however, that in several cases of heterogeneously catalyzed reactions, electron transfer mechanisms are involved but there is no net electron transfer between the two phases. Thus, the potential across the interface is a variable in the expression for the rate constant for the electrocatalytic reaction. The electrocatalyst has a positive or negative effect on enhancing the chemical rate constant and often on altering the reaction path and the intermediate and rate-determining steps for the reaction.

2.8.2.2. *Wide Range of Reaction Rates Attained by Altering the Potential across the Interface at Constant Temperature.* Because of the fact that for most charge-transfer reactions there is an exponential dependence of the current density on potential, it is possible for several electrocatalytic reactions to attain reaction rates covering more than two orders of magnitude on the same electrocatalyst at constant temperature. In the case of heterogeneous catalytic reactions, the only variables for enhancing the rates on the same catalysts are temperature and the concentrations of the reactants. These also influence the rates of electrocatalytic reactions.

2.8.2.3. *An Electrochemical Pathway for Chemical Reactions.* There are a wide variety of chemical reactions, which can also occur via electrochemical pathways. An example of relevance to fuel cells, the combustion of methane to produce CO_2 and water can be carried out at a relatively high temperature catalytically or at a relatively low temperature electrochemically:

Chemical: $$CH_4 + 2O_2 \rightarrow CO_2 + 2H_2O \tag{2.120}$$

Anode: $$CH_4 + 2H_2O \rightarrow CO_2 + 8H^+ + 8e_0^- \tag{2.121}$$

Cathode: $$2O_2 + 8H^+ + 8e_0^- \rightarrow 4H_2O \tag{2.122}$$

The overall reaction that occurs electrochemically is the same as that occurring chemically, as described by Eq. (2.121). The advantage of the electrochemical route is that in addition to the chemical products, electricity is directly generated, while in the case of the combustion route, the conversion of the heat energy (released by

the reaction expressed by Eq. 2.121) to electrical energy has to occur in a subsequent step in a thermal power plant. It is noteworthy to mention that the German expression for fuel cells is *Kalte Verbrennung* (i.e., cold combustion) because fuel cells can directly convert chemical to electrical energy at low temperatures, while high temperatures are necessary for thermal power plants.

2.8.2.4. *Different Products in Different Ranges of Potential.* In electrocatalysis, it is possible to carry out selective oxidation or reduction reactions in different ranges of potential across the electrode/electrolyte interface on the same electrode material under isothermal conditions. For such types of reactions to take place in heterogeneously catalyzed reactions, the only variables are the operating conditions (temperature and pressure) or concentration of reactants. The simplest example of the former is the reactions occurring on a platinum electrode in an aqueous medium. Under these conditions hydrogen evolution occurs at a potential below 0.0 V/RHE, an oxide starts forming at about 0.8 V/RHE, and oxygen evolution occurs above 1.5 V (note that oxygen is not significantly evolved in the potential range 1.23–1.5 V because of the high irreversibility of the reaction). Another good example is the progressive reduction of nitrobenzene on a platinum electrode according to the following reaction:

$$C_6H_5NO_2 + 2e_0^- \rightarrow C_6H_5NO + 2e_0^- \rightarrow C_6H_5NHOH + 2e_0^- \rightarrow C_6H_5NH_2 \tag{2.123}$$

Nitrobenzene $\rightarrow$ Nitroso-benzene $\rightarrow$ Hydroxylamine $\rightarrow$ Aniline

2.8.2.5. *Change in Path of Reactions Using Redox Systems.* The electrooxidation of methanol has a high overpotential on even the most active electrocatalyst (Pt-Ru) with an overpotential of about 400 mV at a current density of 300 mA cm^{-2} at 80 ^{0}C in a DMFC. However, the reaction pathway for the electrooxidation of methanol could be altered with a significant acceleration of the reaction rate by using a redox system. An example is the electrooxidation of the species Mo^{5+} (present in the electrolyte), at the electrode/electrolyte interface to Mo^{6+}, according to the following reaction:

$$Mo^{5+} \rightarrow Mo^{6+} + e_0^- \tag{2.124}$$

and the chemical oxidation of methanol by the Mo^{6+} near the electrode as:

$$CH_3OH + H_2O + 6Mo^{6+} \rightarrow CO_2 + 6H^+ + 6Mo^{5+} \tag{2.125}$$

2.8.2.6. *In-Situ Reactivation of Electrocatalysts.* One of the problems encountered in heterogeneous catalysis is the poisoning of catalyst surfaces by intermediate species and/or byproducts and/or impurities. Poisoning problems arise in electrocatalytic reactions, especially those involving organic reactants and

impurities such as CO. In the case of heterogeneous catalytic chemical reactions, for the regeneration of active sites, it is often possible to stop the reaction periodically and give the catalyst high-temperature heat treatments. In an electrochemical cell, it is possible to regenerate the electrocatalytic sites periodically by the application of electric pulses to either oxidize some organic impurities or to reduce the films (i.e., oxide films) formed on the surfaces.

2.8.2.7. *Electrochemical Nature of Biological Reactions.* In heterogeneous biochemical reactions occurring in living systems, enzymes serve as the catalysts. Most enzyme reactions occur via electron transfer reactions and a more appropriate term for these catalysts is *bioelectrocatalysts*. In several biocatalyzed reactions, proton transfer also occurs. The turnover rates for enzymatic reactions (i.e., the number of individually catalyzed events that occur per active site per sec) are several orders of magnitude (may be as high as six) higher than for heterogeneously catalyzed chemical reactions. Further, their specificities for reactions can be very high, for instance, the enzyme glucose oxidase oxidizes α-glucosidic but not β-glucoside bonds. Enzymes are giant molecules compared to inorganic or organic species involved in electrochemical reactions. For example, cytochrome-C, a relatively small molecule, has a molecular weight of 12,400. In spite of its relatively large size, electron transfer occurs in this enzyme through the modifier to the heme group at a rate about as fast as in a redox reaction involving oxidation of a metallic ion in solution from a lower to a higher valence state.

2.8.3. Similarities Between Electrocatalysis and Heterogeneous Catalysis

2.8.3.1. *Effect of Geometric Factors.* The term *geometric factors* of catalysts refers to their structural and morphological aspects, which include the heterogeneity of surfaces. Also included in the geometric factors are crystal orientation and lattice spacing, crystal defects such as edges, steps and kinks, particle size, and amorphous nature (amorphicity). An original hypothesis for the importance of geometric factors of the catalysts on the rates of reactions was proposed by Balandin.[23] It indicates that reactants and/or intermediates must be sufficiently strongly adsorbed on the surface to accelerate the reaction, but not be too strongly adsorbed to hinder the rate of the subsequent intermediate step. Interatomic distances and crystal structure in the catalyst are critical parameters for the adsorption of a reactant. According to Balandin, bonds between atom in the reactant molecules are weakened, distorted, and in the limiting case may undergo rupture, as illustrated in Figure 2.19, for a reaction of the type:

$$A\,B + C\,D \rightarrow A\,D + BC \tag{2.126}$$

The catalytic activity depends on lattice spacing and structure. The first supporting evidence for the Balandin hypothesis was found that when the

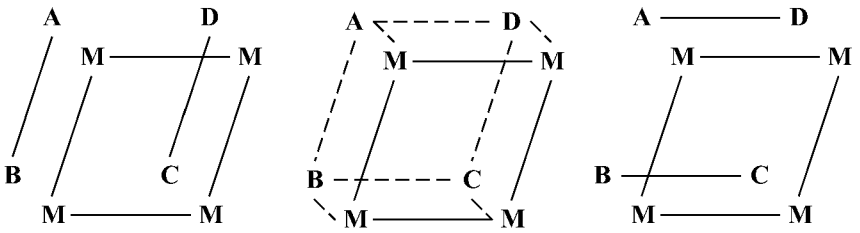

Figure 2.19. Reaction sequence for heterogeneously catalyzed reaction AB + CD and AD+ BC. M's represent metal atoms. Reprinted from J. O'M Bockris and S. Srinivasan, *Fuel Cells: Their Electrochemistry*, Copyright © 1969, with permission from McGraw-Hill Book Company.

hydrogenation benzene and its reverse reaction were considerably more active on catalysts with face-centered cubic or with close-packed hexagonal than with body centered cubic structures. In electrocatalysis, it has been shown that hydrogen evolution has a higher exchange current density on the (111) crystal plane than on its (100) or (111) crystal planes. The reasons why defects in crystals—such as edges, kinks, and steps—play a role in heterogeneous catalysis or electrocatalysis are that the free energies of adsorption reactants/intermediates are higher at these sites because of their intrinsic nature, as well as their having higher coordination numbers of surrounding atoms than those for a planar site. Particle sizes and intersite distances also play significant roles in heterogeneous and electrocatalysis. For example, the rate of oxygen reduction in PAFCs has a practically constant value for Pt particles above 20 to 30 Å, but there is a decrease in rate for smaller particles. Point defects (vacancies and impurities) affect catalytic activities. An example is that the rate of electrolytic hydrogen evolution is higher on an iron electrode, containing 0.2 % carbon than on zone-refined iron with less than 0.01 % impurities. Line defects (dislocations) do not seem to affect rates of fuel cell reactions.

2.8.3.2. *Electronic Factors*. Heterogeneous catalytic and electrocatalytic reactions invariably involve the intermediate steps of adsorption/desorption in the overall reaction. Since the bonds formed between the catalysts and the reactants/intermediates are covalent, these bonds are relatively strong (unlike physical adsorption of molecular hydrogen or oxygen on surfaces). It has for a long time been recognized, first in heterogeneous catalysis and considerably later in electrocatalysis, that transition metals and their alloys are the most active catalysts. In the short space available for this section, it is impossible to summarize the voluminous, innovative research findings to unravel the role of electronic factors of the materials in catalysis and electrocatalysis. One statement, which can support all these findings, is that relative strong covalent-chemical bonds (covalent) are formed between atoms in the catalyst, or in the electrocatalyst, and those in the adsorbed species. As stated in the previous Section, these bonds should be strong enough to

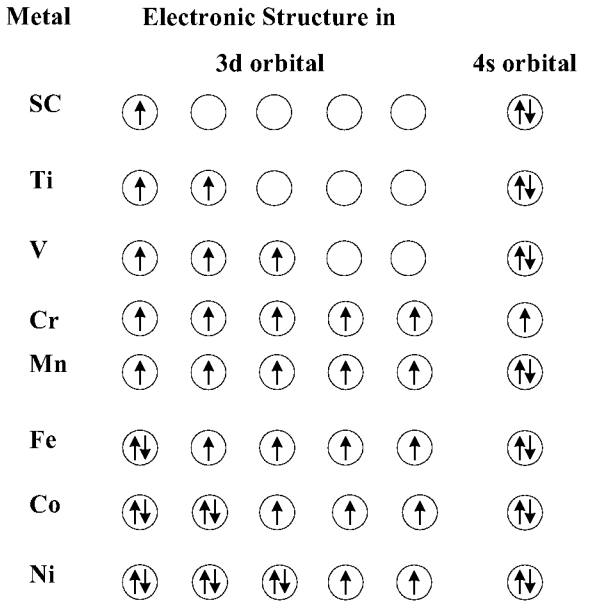

Figure 2.20. The electronic structures for the 3d and 4s orbitals for the transition metals in the first long period of the periodic table. Reprinted from J. O'M Bockris and S. Srinivasan, *Fuel Cells: Their Electrochemistry*, Copyright © 1969, with permission from McGraw-Hill Book Company.

accelerate the formation of these intermediates in the overall reaction but not too strong to have the inhibiting effect of decelerating the subsequent desorption steps of the reaction.

There are two electronic properties that affect the rates of catalytic/electrocatalytic reactions: *d-band vacancies* (a related parameter is the percentage d-band character), and the *work function* of the metal. The transition metals have unpaired d-electrons and their number could vary from one to ten (note that there are 5d orbitals in the two long periods of the periodic table). The electronic structure of the 3d and 4s orbitals for the transition metals in the first long period are shown in Figure 2.20.

The metals Fe, Co, and Ni have 4, 3, and 2 unpaired d-electrons, respectively, in the gaseous phase. However, the situation is different in the metallic state. In the latter state, according to the electron-band theory of metals, there is an electron

overlap of the d-levels with the immediately higher s-level (in the case of the above three metals, these are the 3d and 4s levels). For Ni, with 12 spaces available for electron occupancy in the 3d and 4s levels, 0.54 rather than 2 electrons enter the 4s level. This value is close to the measured value of the saturation magnetic moment of the metal for Ni (0.61 Bohr magnetons).

A parameter related to the d-band vacancy is the *percentage d-band character*. This arises out of Pauling's valence band theory of metals.[24] According to this theory, promotion of electrons to higher orbitals (e.g., 3d to 4s) plays a role in the bonding of metals. In turn, for the metals in the first long period, 4s levels could be promoted to the 4p states and the electronic structure in the solid state involve the 3d, 4s, and 4p states. This process is referred to as *dsp hybridization*. The percentage d-band character is defined as the extent to which dsp hybridization occurs. Table 2.2 illustrates the percentage d-band character of the transition metals in the first, second, and third long periods of the periodic table. Metals, having more unpaired electrons in the d-band, have a lower percentage d-band character.

The question that one might now ask is what does heterogeneous catalysis/electrocatalysis have to do with this. The answer is apparent from the preceding section: catalytic reactions involve intermediate steps of adsorption/desorption via covalent bonds. For such type of bond formation, the catalyst plays the role of being a donor or acceptor of electrons to or from the adsorbed atoms or molecules. For an adsorption reaction, a metal with a lower percentage d-band character (i.e., more unpaired electrons) is more favorable; for a desorption reaction, it is the reverse case.

Another electronic factor, which has proven to be very beneficial in a fundamental understanding of heterogeneous catalysis/electrocatalysis and tailor-making novel catalytic materials, is the *work function* (φ) of the metal. The work function of a metal is defined as the energy required to remove an electron from its bulk to a point well outside it. Even though the work function is a bulk property of the metal, it is strongly affected by the surface because the transfer of the electron, from the bulk of the metal to a point well outside it, involves its passage across the metal/vacuum interface. For the transition metals, it has been found that the work function increases with the d-band character because with increasing d-band character, the number of unpaired electrons decreases, making it more difficult to extract an electron out of the metal. From a catalytic point of view, it would then

TABLE 2.2

Percentage *d*-Band Character in the Metallic Bond of Transition Elements[a]

Sc	Ti	V	Cr	Mn	Fe	Co	Ni	Cu
20	27	35	39	40.1	39.5	39.7	40	36
Y	Zr	Nb	Mo	Tc	Ru	Rh	Pd	Ag
19	31	39	43	46	50	50	46	36
La	Hf	Ta	W	Rh	Os	Ir	Pt	Au
19	29	39	43	46	49	49	44	

[a]From Suggested Reading 1.

follow that the enthalpy of adsorption of a species will decrease with an increase of the percentage of the d-band character and an increase of the work function of the metal.

A third electronic factor, which is useful in understanding its effect in heterogeneous catalysis/electrocatalysis is the *electronegativity* of an element (χ). Pauling proposed an empirical equation for the bond energy of say $D_{M\text{-}H}$, a hydrogen atom (H) adsorbed on a metal (M) by the equation:

$$D_{M-H} = 0.5\left(D_{M-M} + D_{M-H}\right) + 23.06\left(\chi_{M-}\chi_{H}\right)^2 \qquad (2.127)$$

where $D_{M\text{-}M}$ and $D_{M\text{-}H}$ are the bond dissociation energies of two neighboring metal atoms and of the hydrogen molecule, respectively. The parameters χ_M and χ_H are the electronegativities of the metal and hydrogen atom, respectively.

In Chapter 6, the roles of the aforementioned electronic factors influencing electrocatalysis of fuel cell reactions are addressed. The reader is referred to the voluminous literature for analyses of heterogeneously-catalyzed reactions.

2.8.4. At What Potentials Should One Compare Reaction Rates to Elucidate the Roles of Electronic and Geometric Factors?

This topic has been discussed over the last 40 years. Should we compare the reaction rates at the reversible potential or at the potential of zero charge of the metal? If the transfer coefficients (α) are the same for the electrochemical reaction on different electrocatalysts, the accepted view is that the exchange current density is a reasonably good measure of inherent electrocatalytic activity; however, if the transfer coefficients are different, causing a change in Tafel slope with increasing current density, it is more desirable to make comparisons at desired overpotentials. The current density at the potential of zero charge, reveals an inherent activity of the metal, devoid of any electrical aspects of the double layer. Knowledge of the influence of the potential across the interface on the rate of an electrochemical reaction is a valuable and additional diagnostic criterion for determining the mechanism of an electrochemical reaction.

2.9. ADSORPTION ISOTHERMS AND PSEUDOCAPACITANCE

2.9.1. Types of Adsorption Isotherms and Their Influence on Electrode Kinetics and Electrocatalysis

2.9.1.1. *Langmuir Isotherm.* In heterogeneous catalysis involving multi-step reactions at solid/gas or solid/liquid interfaces, as well as in multi-step charge-transfer reactions, the adsorption and desorption of reactants and intermediate species play a dominant role. This is more so for reactions in which the solid phase

serves a catalytic/electrocatalytic role. The kinetics of the adsorption/desorption steps depends on the physicochemical characteristics of the solid phase (e.g., geometric and electronic factor, and the availability of free sites on the surface.) In the case of electrocatalytic reactions, the intermediate adsorption/desorption steps may or may not involve electron transfer. Chemical steps may precede or succeed the charge transfer step. The kinetics of the adsorption/desorption steps strongly depends on the types of isotherms governing the processes. There are also cases where diffusion of the species plays a role. Knowledge of the type of isotherm and the kinetics of the adsorption/desorption step is vital in elucidating the mechanism of several types of electrochemical reactions, particularly gas-evolution/gas-consumption reactions (as in water electrolysis and fuel cells) and electroorganic oxidation and reduction reactions.

Sections 2.1.2. and 2.1.3. provided a brief description of types of adsorption isotherms and of the effects of the adsorption of ions and of neutral molecules on the structure of the double layer. Of the different types of isotherms considered in these sections, the two most common ones are the Langmuir and the Temkin adsorption isotherms. In this section, an analysis will be made of the kinetics of a two-step electrochemical reaction, which involves an adsorption/desorption step of an intermediate governed by the Langmuir isotherm.

Let us consider an electrochemical reaction of the type:

Step1 $$M + A^- \rightleftharpoons MA + e_0^- \tag{2.128}$$

Step 2 $$2MA \rightleftharpoons 2M + A_2 \tag{2.129}$$

Overall Anodic $$2A^- \rightarrow A_2 + 2e_0^- \tag{2.130}$$

where M is the electrocatalyst. A^- is the ion in solution (e.g., a chloride ion), MA is the adsorbed intermediate and A_2 is the product (e.g., Cl_2). According to the Langmuir-isotherm kinetics, the free sites on the surface of the electrocatalyst determine the rate of the first step of the adsorption v_1, while the rate of the reverse reaction, v_{-1}, is dependent on the coverage of this species. Thus,

$$v_1 = k_1 c_A (1-\theta) \exp \frac{\beta VF}{RT} \tag{2.131}$$

and

$$v_{-1} = k_{-1} \theta \exp \frac{-(1-\beta)VF}{RT} \tag{2.132}$$

In the above equations, k_1 and k_{-1} are rate constants for the forward and reverse steps, respectively, θ is the fractional coverage of the surface by the intermediate MA, V is the potential across the electrode/electrolyte interface, and β is the symmetry factor. The rates of the second step in the forward and reverse directions, respectively, ν_2 and ν_{-2}, are given by:

$$\nu_2 = k_2\theta^2 \tag{2.133}$$

and

$$\nu_{-2} = k_{-2}(1-\theta)^2 P_{A_2} \tag{2.134}$$

where k_2 and k_{-2} are the respective rate constants and P_{A_2} is the pressure of the product gas. It must be noted that since this second step does not involve electron transfer, it is not directly dependent on the potential across the interface. However, since the fractional coverage, θ, is dependent on potential, there is an indirect dependence of the rates (forward and backwards) on potential, as will be seen by the following analysis. Suppose one assumes that the second step (Eq. 2.129) is rate determining in the anodic-gas evolution reaction (Eq. 2.130). Then, one may consider that the first intermediate step is in equilibrium and obtain an expression for θ as:

$$\theta = \frac{K_1 c_{A^-} \exp\dfrac{VF}{RT}}{1 + K_1 c_{A^-} \exp\dfrac{VF}{RT}} \tag{2.135}$$

where $K_1 = k_1/k_{-1}$.

The Langmuir-adsorption isotherm is applicable at very low or very high coverage of the adsorbed species. If we assume the case of $\theta \rightarrow 0$, then:

$$\theta = K_1 c_{A^-} \exp\frac{VF}{RT} \tag{2.136}$$

When the second forward step is the rate-determining step, its rate is:

$$\nu_2 = k_2 K_1^{\,2} \exp\frac{2VF}{RT} \tag{2.137}$$

and since $(1 - \theta) \approx 1$, the rate of the reverse step is:

$$v_{-2} = k_{-2} P_{A_2} \tag{2.138}$$

From this overall rate, it is clear that with the assumptions made, the Tafel slope for the gas evolution reaction is $RT/2F$, while the reverse reaction rate is independent of potential and depends only on pressure of the gas A_2. In Chapter 5, a more detailed analysis of the electrode kinetics of electrolytic hydrogen evolution/ionization reactions will be made. It will be based on the Langmuir adsorption isotherm of the intermediate. The hydrogen electrode reaction is analogous to the above type of reaction but it is in the reverse electrochemical direction (i.e., gas evolution is the cathodic reaction and gas consumption is the anodic one).

2.9.1.2. *Temkin Isotherm.* It was stated in Sections 2.1.2. and 2.1.3. that the Langmuir isotherm is based on the availability of free sites on the electrode. This type of behavior is mostly applicable at low and high coverage ($\theta \rightarrow 0$) and ($\theta \rightarrow 1$). However, in the case of several electrochemical reactions, particularly electroorganic oxidation (as in fuel cells using organic fuels directly) and reduction reactions (electrosynthesis), as well as the oxygen-electrode reaction (as in water electrolysis or fuel cells), intermediate species are adsorbed to a relatively high extent. The availability of free sites is not the only factor that governs the adsorption of the reactant or intermediate species. As stated in Section 2.1.2., the Temkin isotherm represents such types of behavior. The free energy of adsorption (ΔG_{ads}) is then dependent on lateral interaction between the adsorbed species and the heterogeneity of the surface. In most cases, it was found that there is a linear relation between ΔG and θ. Thus, one may write:

$$\Delta G_0^{\,0} = \Delta G_0^{\,0} + r\theta \tag{2.139}$$

where $\Delta G_\theta^{\,0}$ and $\Delta G_0^{\,0}$ are the standard free energies of adsorption at coverage values of $\theta = \theta$ and $\theta = 0$, and r is an interaction-energy parameter.

We shall now examine how the adsorption behavior of a Temkin-isotherm type of the intermediate, MA, affects its electrode kinetics. Taking into consideration the variation of the standard free energy of adsorption with coverage, as expressed by Eq. (2.139), the rates of the forward and backward intermediate steps will be given by:

$$v_1 = k_1(1-\theta)c_{A^-} \exp\left(\frac{\beta VF}{RT}\right)\exp\left(\frac{-\gamma r\theta}{RT}\right) \tag{2.140}$$

and

$$v_{-1} = k_{-1}\theta \exp\left[-(1-\beta)\frac{VF}{RT}\right]\exp\left[(1-\gamma)\frac{r\theta}{RT}\right] \tag{2.141}$$

The second exponential term in each of the above equations represent the changes in the activation energies for these reactants as a result of the change in adsorption energy of the species MA with coverage. The term γ is analogous to the symmetry factor. An approximation is made that in the range of $0.2 < \theta < 0.8$, the variations in the linear terms of θ are considerably less than those in the exponential terms of θ. Thus, Eqs. (2.140) and (2.141) may be reduced to:

$$v_1 = k_1 c_A \exp\left(\frac{\beta VF}{RT}\right)\exp\left(\frac{-\gamma r\theta}{RT}\right) \tag{2.142}$$

$$v_{-1} = k_{-1}\exp\left[(1-\beta)\frac{VF}{RT}\right]\exp\left[(1-\gamma)\frac{r\theta}{RT}\right] \tag{2.143}$$

The rates of the second forward and reverse steps are:

$$v_2 = k_2\theta^2 \exp\left(\frac{2\gamma r\theta}{RT}\right) \cong k_2 \exp\frac{2\gamma r\theta}{RT} \tag{2.144}$$

and

$$v_{-2} = k_{-2}(1-\theta)^2 \exp\left[-2(1-\gamma)\frac{r\theta}{RT}\right] \cong k_{-2}\exp\left[-2(1-\gamma)\frac{r\theta}{RT}\right] \tag{2.145}$$

If we assume that the second step is rate determining and the first step is virtually in equilibrium, the rate of the overall forward and backward directions will be given by

$$v_2 = k_2\left(k_1 c_{A^-}\right)^2 \exp\frac{2\gamma rF}{RT} \tag{2.146}$$

and

$$v_{-2} = k_{-2}\left(\frac{1}{K_1 c_A}\right)^{-2(1-\gamma)} \exp\left[-2(1-\gamma)\frac{VF}{RT}\right] \tag{2.147}$$

Since the currents are proportional to the velocities:

$$\frac{\partial V}{\partial \ln i_2} = \frac{RT}{2\gamma F} \tag{2.148}$$

and

$$\frac{\partial V}{\partial \ln i_{-2}} = \frac{RT}{2(1-\gamma)F} \tag{2.149}$$

An examination of our analyses of the same reaction, governed by the two types of adsorption isotherms, reveals their influence on the electrode kinetics, including the dependence of the reaction rates on potential.

The mechanism of the oxygen-electrode reaction (evolution, as during water electrolysis, and consumption, as in fuel cells) well exemplifies the influence of the Langmuir type and Temkin type of adsorption of the intermediate M–O or M–OH (where M is the electrocatalyst on the electrode kinetics). This aspect is dealt with in detail in Chapter 5.

2.9.2. Adsorption Pseudocapacitance

2.9.2.1. *What is Pseudocapacitance?* The topics of the structure of the double layer and the variation of its capacity with potential as well as the effects of adsorption of ions and neutral molecules were dealt with in Section 2.1. In the preceding Section, we analyzed effects of the types of isotherms on the electrode kinetics of the reactions. Another important characteristic of certain types of electrochemical reactions, including fuel cell reactions, is their exhibition of another type of capacitance, namely *adsorption pseudocapacitance.* Adsorption pseudocapacitance is defined as the differential capacitance of an electrode/electrolyte interface caused by the change in coverage of an electroactive species with potential across the interface. It is usually observed in an electrochemical reaction in which a charge transfer step precedes the rate-determining step. One of the best examples is the electrolytic hydrogen evolution reaction in which the first electron transfer step to form the MH species is fast, and the second step involving the combination of two hydrogen atoms to form the hydrogen molecule is slow (see Eqs. 2.52 and 2.59). In such a case, pseudocapacitance is observed during transient studies, as in cyclic voltammetry or during switching on and off the current. The pseudocapacitance is a measure of the change in charge with potential. The charge is related to the coverage θ by the expression:

$$q = q_0\theta \tag{2.150}$$

where q_0 is the charge at $\theta = 1$. The differential capacitance, i.e., the pseudocapacitance, C_{ps}, is expressed by:

$$C_{ps} = \left(\frac{\partial q}{\partial V}\right) = q_0\left(\frac{\partial \theta}{\partial V}\right) \tag{2.151}$$

2.9.2.2. *Theoretical Analysis of Dependence of Pseudocapacitance on the Type of Adsorption Isotherm.* The Langmuir type adsorption of an intermediate in a reaction is represented by Eq. (2.136). Using Eq. (2.135) in Eq. (2.150) one can show that the expression for C_{ps} is:

$$C_{ps} = \frac{q_0 F}{RT}\theta(1-\theta) \tag{2.152}$$

It can also be shown by analysis of this expression that C_{ps} has a maximum at $\theta = 0.5$, which is given by the equation:

$$C_{ps} = \frac{q_0 F}{4RT} \tag{2.153}$$

A plot of C_{ps} vs. θ will reveal a parabolic behavior symmetrical around $\theta = 0.5$. The expression for C_{ps} as a function of potential for this case is

$$C_{ps} = \frac{q_0 F}{RT}\frac{c_{A^-} K_1 \exp\dfrac{VF}{RT}}{\left(1 + c_{A^-} K_1 \exp\dfrac{VF}{RT}\right)^2} \tag{2.154}$$

A plot of C_{ps} vs. potential for hydrogen adsorption on platinum is shown in Figure 2.21. For this case, with 10^5 atomic sites of Pt cm^{-2}, the maximum value of C_{ps} (i.e., at $\theta = 0.5$) is 1.6×10^3 $\mu F\ cm^{-2}$. This value is considerably higher (by a factor of 100) than the double layer capacity at an ideally polarizable interface, which behaves very much like a solid-state capacitor. It is for this reason that electrochemical capacitors are referred to as supercapacitors and are gaining interest for applications such as high power density energy storage devices (c.f. Chapter 3).

We shall now analyze the pseudocapacitance-potential behavior for the case of adsorption of the intermediate species governed by the Temkin isotherm. From the derivation of the expression for θ for this isotherm, and Eq. (2.151), it follows that:

$$\frac{q_0}{C_{ps}} = \frac{dV}{d\theta} = \frac{RT}{F} d\ln\frac{\theta}{1-\theta} + \frac{r}{F} \tag{2.155}$$

From the above equation and Eq. (2.153), one may arrive at the expression:

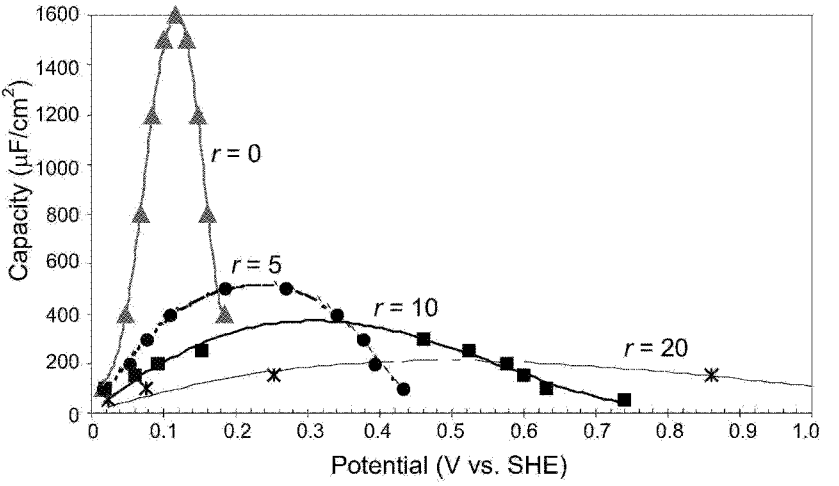

Figure 2.21. Plots of pseudocapacitance versus potential for hydrogen adsorption/desorption on platinum for different values of the heterogeneity parameter, r. The case $r = 0$ is for Langmuir conditions of adsorption/desorption and the cases $r > 0$ are for Temkin conditions.Reprinted from B. E. Conway and E. Gileadi, Transactions of the Faraday Society **58**, 2493, Copyright © 1962, with permission from The Royal Society of Chemistry.

$$\frac{1}{C_{ps}} = \frac{1}{C_L} + \frac{1}{C_T} \tag{2.156}$$

This equation shows that the pseudocapacitance is a series combination of two capacitors: one as in Langmuir case, C_L, and the other involving the heterogeneity parameter. Plots for the variation of C_{ps} with potential V are also shown in Figure 2.21 for different r values. The case $r = 0$ represents Langmuir adsorption behavior. With increasing values of r, there is a decrease in peak height as well as a broadening of the parabolic curves. For $r \neq 0$, the capacitor maximum is given by:

$$C_{ps,M} = \frac{q_0 F}{4RT + r} \tag{2.157}$$

Knowledge of the dependence of the pseudocapacitance on potential is a useful diagnostic criterion for the determination of the mechanism of an electrochemical reaction (i.e., whether Langmuir or Temkin type adsorption prevails). This is quite applicable to the electrooxidation of hydrogen and of organic fuels as well as electroreduction of oxygen in fuel cells.

2.9.2.3. *Electrical Equivalent Circuits for Reactions Exhibiting Pseudocapacitances.* An experimental technique that has been gained momentum since the 1970s to elucidate the mechanism of several types of electrochemical reactions is Electrochemical Impedance Spectroscopy (EIS). In order to analyze the results of the EIS experiments, the most commonly used method is that based on an equivalent circuit for the reaction being investigated. The rationale for bringing up this topic is that EIS is one of the most valuable transient methods for investigating mechanisms of reactions, which exhibit pseudocapacitance. For the reaction sequence considered in the preceeding Sections, the equivalent electrical circuit generally used is shown in Figure 2.22, where C_{DL} represents the double-layer capacity, C_{ps} the pseudocapacity for the charge transfer step, R_{CT} the charge transfer resistance of this step, and R_{rec} the reaction resistance for the recombination step. By an analysis of the EIS experimental results for this reaction using this type of equivalent circuit, it is possible to determine the relevant electrode kinetic parameters.

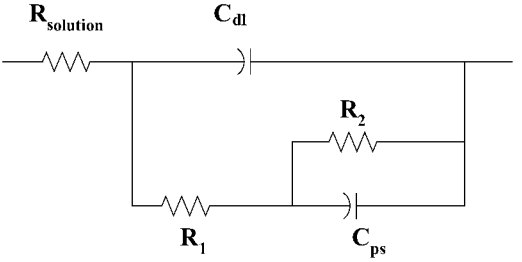

Figure 2.22. Equivalent circuit for the hydrogen evolution reaction according to the (fast discharge)-(slow recombination) mechanism. C_{dl} is the double layer capacity at the electrode/electrolyte interface, C_{ps} is the pseudocapacitance for the hydrogen adsorption/desorption step, R_1 and R_2 are the charge transfer resistance for the fast discharge step and recombination steps, and R is the electrolyte resistance. Reprinted from J. O'M Bockris and S. Srinivasan, *Fuel Cells: Their Electrochemistry*, Copyright © 1969, with permission from McGraw-Hill Book Company.

Suggested Reading

1. J. O'M Bockris and S. Srinivasan, *Fuel Cells: Their Electrochemistry* (McGraw-Hill Book Company, New York, 1969).
2. A. J. Bard and L. Faulkner, *Electrochemical Methods* (Wiley, New York, 1980).

3. C. H. Hamman, A. Hammnett, and W. Vielstich, *Electrochemistry* (Wiley-VCH Verlag GmbH, Weinheim, Germany, 1998).
4. P. M. Natishan (Ed.), *What is Electrochemistry?*, 4th edition (The Electrochemical Society, Pennington, N. J., 1997).

Cited References

1. H. Helmholtz and W. Abhandl, *Physik. Tech. Reichsanst Alt.* **1,** 925 (1879).
2. A. Gouy, *Ann, Chim. Phys.* **29**, 145 (1903); *Compt. ReNd.* **149,** 654 (1909).
3. D. L. Chapman, *Phil. Mag.* **25,** 475 (1913).
4. O. Stern, *Z. Electrochem.* **30,** 508 (1924).
5. O. A. Esin and B. F. Markov, *Zh. Fiz. Khim.* **13,** 318 (1939).
6. D. C. Grahame, *J. Electrochem Soc.* **98,** 313 (1951).
7. M. A. V. Devanathan, *Trans. Faraday Soc.*, **50,** 373 (1954).
8. J. O'M Bockris, M. A. V Devanthan, and K. Mueller, *Proc. Roy. Soc., Ser. A.* **274,** 55 (1963).
9. I. Langmuir, *J. Amer. Chem. Soc.* **40,** 1361 (1918).
10. A. N. Frumkin, *Z. Physik.* **35,** 792 (1926).
11. M. I. Temkin, *Zh. Fiz. Khim.* **15,** 296 (1941).
12. P. J. Flory, *J. Chem. Phys.* **10,** 51 (1942).
13. M. L. Huggins, *Ann. NY Acad. Sci.* **43,** 6 (1942).
14. J. O'M Bockris, M. Gamboa, and M. Szklarczyk, *J. Electroanal. Chem.* **339,** 355 (1992).
15. J. O'M Bockris. M. Green, and D. A. J. Swinkels, *J. Electrochem. Soc.* **11,** 743 (1966).
16. J. O'M Bockris and K. T. Jeng, *J. Electroanal. Chem.* **330,** 541 (1992).
17. W. H. Brattain and C. G. B. Garrett, *Ann. NY Acad. Sci.* **58,** 951 (1954).
18. V. S. Bagotzky and Y. B. Vassilyev, *Electrochim. Acta* **12,** 1323 (1967).
19. J. Christiansen, *Z. Physik. Chem. Ser. B* **33** (1936) 145; **37,** 374 (1937).
20. J. A. V. Butler, *Proc. Roy. Soc. Ser. A* **157,** 423 (1936).
21. R. W. Gurney, *Proc. Roy. Soc. Ser. A* **134,** 137 (1931).
22. W. Nernst and E. S. Merriam, *Z. Physik. Chem.* **53,** 235 (1905).
23. A. A. Balandin, *Z. Physik. Chem.* **B2,** 28 (1929); **B3,** 167 (1929).
24. L. Pauling, *Phys. Rev.* **54,** 899 (1938); *Proc. Roy. Soc. Ser. A* **196,** 343 (1949).

PROBLEMS

1. There has been a progressive advance in elucidating the structure of the electric double layer at an electrode/electrolyte interface starting from the Helmholtz model to the water dipole model. Identify the distinctive features of these Double Layer models.

2. What is the main difference between the structure of the double layer at (i) a metal/electrolyte interface, and (ii) a semiconductor/electrolyte interface?

What is the common feature in the space charge region of the semiconductor and in the diffuse-layer region in the electrolyte?

3. What are adsorption isotherms? How do these isotherms affect the structure of the double layer in the case of (i) specific adsorption of ions, and (ii) adsorption of neutral organic molecules (in this case consider both polar and non-polar molecules)?

4. Express the overall electrochemical reactions, as equations, for the following reference electrodes:
   (a) Reversible hydrogen electrode
   (b) Calomel electrode
   (c) Silver/silver chloride electrode
   (d) Mercury/mercuric oxide electrode
   Reference electrodes are also referred to as *ideally non-polarizable electrodes*. What is the reason for this terminology from an electrode kinetic point of view? (Hint: What will be the order of magnitude values of the exchange current densities for these reference electrodes?).

5. The cathodic reduction of nitrobenzene to aniline follows a consecutive reaction path (see Eq. 2.123). It is also possible to have intermediate reaction products by partial reduction of C_6H_5NO and C_6H_5NHOH. Express the equations leading to these products by complete or partial reduction. What is the reason for referring to the electrode at which these reactions occur as a non-polarizable electrode? Explain it in terms of probable values for their exchange current densities.

6. Examine Figure 2.12, *Typical plot of free energy* vs. *distance along reaction path for a consecutive reaction*. What is the reason for the intermediate step from C to D for the forward reaction and from D to C for the reverse reaction being the rate-determining step (rds)? With these being their rds, derive the expressions for the velocities of the forward reactions, assuming that the steps from A to C and F to D are in equilibrium.

7. In a reaction occurring by the consecutive pathway, the rate-determining step (rds) is the slowest one in the sequence of intermediate steps. What is the rds in a reaction that occurs by the parallel reaction pathway? Give an example of a reaction that occurs by this route. What type of reaction is referred to as a coupled reaction?

8. Take into consideration electrolytic hydrogen evolution. It occurs via the reaction path, as expressed by the proton discharge step according to Eq. (2.52), and is followed by the recombination step according to Eq. (2.59). Assuming that the proton discharge step is the rds step, what are the physico-chemical characteristics that have to be taken into account in constructing the *potential energy* vs. *distance from electrode surface* plots?

9. Assuming the expression represented by Eq. (2.92) for the dependence of overpotential on current density, construct the Tafel plots for the following cases:
   a) Slow discharge–fast recombination: for the high overpotential metal electrodes (e.g., mercury, lead, thallium), i_o is about 10^{-10} A cm^{-2}, and the transfer coefficient is 0.5. Construct the overpotential vs. current density plot for values of η in the range 10 to 500 mV.
   b) For the medium overpotential metals (e.g., Fe, Ni, Cu), the electrochemical desorption step, i_o, is about 10^{-6} A cm^{-2}, and $\alpha = 1.5$ up to a current density of 100 mA cm^{-2}. Above this current density, $\alpha = 0.5$ and $i_0 = 10^{-4}$ A cm^{-2}.
   c) Fast discharge–slow recombination: for the low overpotential metals (e.g., Pt, Rh, Ir), assume $i_o = 10^{-3}$ A cm^{-2} and $\alpha = 2$. Make all of these plots on one sheet of paper and propose some comments as to which type of electrode material will be best for a fuel cell application. Also, at what values of overpotential can the current density for the reverse reaction be less than 5% of that for the forward direction so that the former can be neglected in the expression for i as a function of η (Eq. 2.92)? What will then be the equation for i as a function of current density? What is this plot referred to as and what is the name of the scientist who used it empirically in 1905?

10. For what reason is the quantum mechanical treatment better than the classical for electron transfer reactions? (Hint: Read Section 2.5.2. before you answer this question).

11. At what values of overpotential can the exponential terms in Eq. (2.92) be linearized for the three cases in Problem 6? For these cases, what does the expression for i as a function of η reduce to?

12. What are the expressions for the charge transfer resistance as derived from the expressions for i as a function of current density using (i) Eq. (2.93) and (ii) Eq. (2.95)? For the three cases considered in Problem 6, plot the charge transfer resistance as a function of current density. What is the significant difference in the characteristics considering cases a and b on one hand and case c on the other for the charge transfer resistance as a function of current density?

13. What is meant by the term *mass transport overpotential*? Using values of $i_L = 10^{-4}$ A cm^{-2}, $n = 2$, 100 mV $\leq \eta_D \leq$ 500 mV, and $T = 25$ °C in Eq. (2.109), plot i as a function of η_D on a semi-logarithmic scale (i vs. log η) and linear scale (i vs. η). Then, plot mass transport resistance ($d\eta_D/di$) vs. i. What specific features do you visualize at low and high current density? At what values of η_D can Eq. (2.109) be linearized?

14. What is *ohmic overpotential*? What are the main contributions to ohmic overpotential?